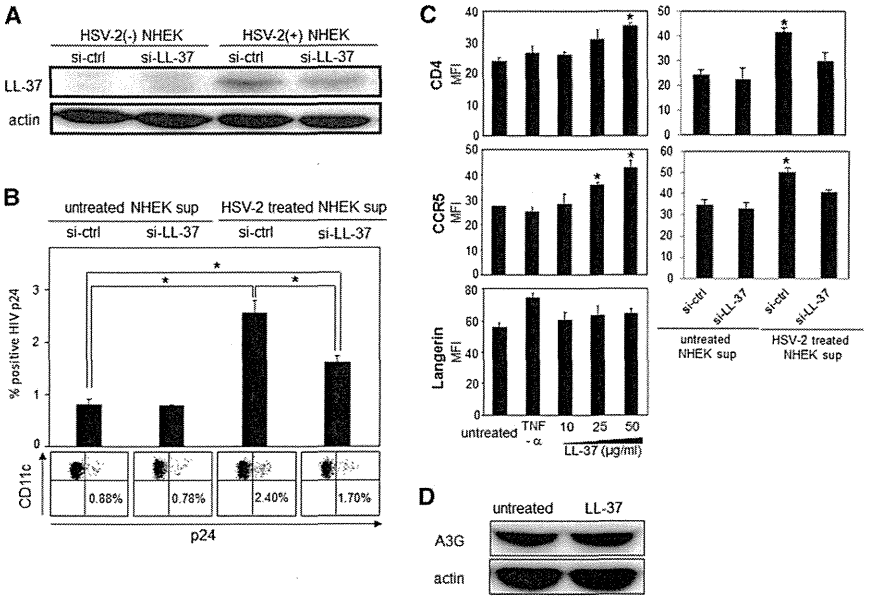

Figure 4. Silencing of LL-37 in HSV-2-Infected NHEKs Abrogates Enhanced HIV Infectivity in mLCs

(A) NHEKs were transfected with control or LL-37 siRNA and then exposed with or without HSV-2. Cells were lysed and then determined the expression of LL-37 by western blot analysis.

(B) mLCs were incubated with indicated culture supernatants for 12 hr and then exposed to R5 HIV. mLCs were collected 7 days after the HIV exposure, and HIV p24$^+$ cells were assessed in langerin$^+$ CD11c$^+$ mLCs. Representative flow cytometric analyses of CD11c and p24 mAb double-stained cells are shown.

(C) mLCs were stimulated with TNF-α or LL-37 at the indicated concentrations or indicated culture supernatants for 24 hr. The expression of CD4, CCR5, and langerin was assessed by flow cytometry.

(D) The expression of A3G was determined by western blot analysis. Results are shown as means ± SD (n = 3) (*p < 0.05). All data shown represent at least two separate experiments. See also Figure S4.

a dose-dependent manner, but LL-37 did not affect infection with VSV-G (Figure 5A). Consistent with previous findings (Kawamura et al., 2001), mLCs were resistant to X4-VSV, even after LL-37 treatment. These results provide direct evidence that LL-37, which upregulates surface expression of CD4 and CCR5 in LCs, promotes increased R5 HIV entry into these cells. Furthermore, similar effects of LL-37 were observed when mLCs were infected with R5 HIV primary isolates: JR-FL and AD8 (Figures 5B and 5C).

LL-37 Decreases HIV Infectivity in mDCs

We next examined whether LL-37 affects HIV infectivity in non-LC-like DCs. Similar to mLCs, LL-37 significantly upregulated surface expression of CD86 and CCR7 on monocyte-derived DCs (mDCs, Figure S3), indicating that LL-37 induces DC maturation. In marked contrast to mLCs, however, there was inhibition of HIV infection in mDCs when these cells were preincubated with LL-37 prior to HIV exposure (Figure 6A), indicating that LL-37 effects on HIV infectivity are differentially regulated in LCs and DCs. LL-37 did not affect CD4 or A3G expression in DCs but markedly downregulated surface expression of CCR5 and DC-SIGN (Figures 6B and 6C). It has been shown that DC-SIGN binds HIV and plays a critical role for HIV replication in mDCs (Gringhuis et al., 2010). These results, in contrast to mLCs, suggest that decreased HIV infection levels observed in LL-37-treated mDCs may be due to downregulation of DC-SIGN and/or CCR5 on their cell surfaces. Taken together, our results indicated the presence of exclusive machinery to augment HIV infection by LL-37 in LC in contrast to that in CD4$^+$ T cells (Bergman et al., 2007) and mDCs.

LL-37 Enhances HIV Transmission from LCs to CD4$^+$ T Cells

We next examined whether LL-37 affected HIV transmission from LCs to cocultured CD4$^+$ T cells. mLCs or mDCs were stimulated with AMPs or TNF-α for 24 hr, exposed to HIV-1_{Ba-L}, and then cocultured with allogeneic CD4$^+$ T cells for 12 days. Consistent with results showing that LL-37 increases HIV infection levels in mLCs (Figure 3A), preincubation of mLCs with LL-37 significantly enhanced subsequent HIV transmission from mLCs to CD4$^+$ T cells in a dose-dependent manner; preincubation with other AMPs did not affect HIV transmission levels in mLC-T cell cocultures (Figure 7A). By contrast, HIV transmission from mDCs to CD4$^+$ T cells was significantly decreased by preincubation of mDCs with LL-37 (Figure 7B), consistent with decreased HIV infection levels in LL-37-treated mDCs (Figure 6A).

DISCUSSION

LCs are generally believed to be one of the cell types that plays a pivotal role in the dissemination of virus during sexual transmission of HIV. To understand the biologic mechanisms by which HSV-2 increases acquisition of HIV, we tested the hypothesis that HSV-2 modulates LC susceptibility to HIV. As expected, we found that HSV-2 enhances HIV susceptibility of LCs within epithelial tissue (Figure 1), consistent with a recent finding that HSV-2 directly enhances HIV susceptibility in LCs (de Jong et al., 2010). However, in our ex vivo explant model, the percentage of HSV/HIV-coinfected LCs was quite low. Instead, our findings suggested that HSV-2 increases HIV susceptibility in LCs by indirect (i.e., epithelial cell-dependent) mechanisms. More specifically, we show here that LL-37 produced by HSV-2-infected epithelial cells enhances HIV infection of LC, most likely by increasing surface expression of CD4 and CCR5 on these cells.

There are conflicting prior reports on how defensins affect HIV infectivity. A variety of anti-HIV activities for hBD2 and hBD3 have been reported, including direct inhibition of virions, indirect inhibition of HIV replication, and downregulation of HIV coreceptors (Klotman and Chang, 2006; Quiñones-Mateu et al., 2003). By contrast, other studies have shown increased HIV infection of

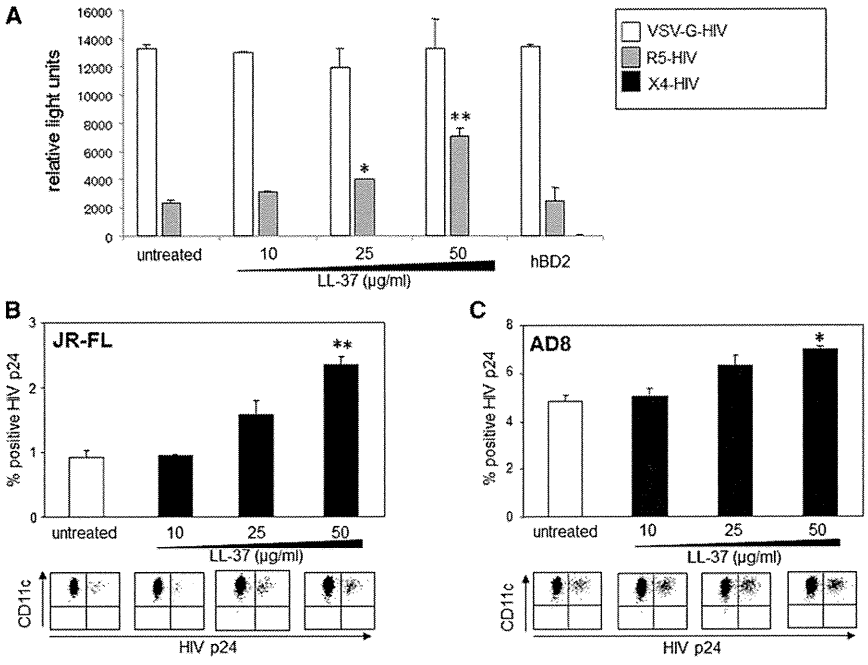

Figure 5. LL-37 Enhances mLCs Susceptibility to R5-HIV and R5 HIV Primary Isolates

mLCs were stimulated with LL-37 at the indicated concentration or hBD2 as control, and then exposed to pseudotyped viruses (R5-HIV, X4-HIV or VSV-G-HIV) for 72 hr (A) or R5 HIV primary isolates (JR-FL or AD8) for 2 hr (B and C). To assess pseudotyped virus infection levels, the average luciferase activity was calculated as relative light units (A). To assess primary HIV infection levels, mLCs were collected 7 days after the HIV exposure, and HIV p24$^+$ cells were assessed in langerin$^+$ CD11c$^+$ mLCs (upper panels, % of positive cells for HIV p24 in langerin$^+$ CD11c$^+$ mLCs; and lower panels, representative flow cytometric analyses following LL-37 stimulation). Results are shown as means ± SD (*$p < 0.05$; **$p < 0.01$). All data shown represent at least two separate experiments. See also Figure S5.

primary CD4$^+$ T cells by HD5 and HD6, and no effects on cell-surface HIV coreceptor expression by hBD1 and hBD2 (Klotman et al., 2008; Sun et al., 2005). These conflicting reports might be due to differences in experimental conditions or cell types used (e.g., PBMC or CD4$^+$ T cells). Interestingly, we found that, unlike PBMC and CD4$^+$ T cells, human β defensins did not affect HIV infectivity of LCs (Figure 3). Although no significant differences were detected, hBD2 and HD5 tended to decrease HIV infectivity of LCs. In addition, consistent with a previous finding that LL-37 inhibits HIV replication in CD4$^+$ T cells (Bergman et al., 2007), we found that LL-37 significantly inhibited HIV infectivity in DCs, probably through downregulation of surface DC-SIGN expression (Figure 6). By contrast, LL-37 upregulated surface expression of CD4 and CCR5 in LCs, and upregulation strongly correlated with the increased R5 HIV entry and infection within these cells (Figure 4 and Figure 5). Thus, these findings clearly indicate that the effects of AMPs on HIV infectivity are differentially regulated depending on the target cell type.

We found that HSV-2 infection in epithelial cells induced the production of soluble LL-37 that had potent enhancing effects on HIV infectivity in LCs. siRNA-mediated interference of LL-37 transcription blocked, at least in part, increased HIV infectivity. We hypothesize that when HSV-2 infection occurs in genital mucosa, LL-37 produced by HSV-infected epithelial cells augments HIV susceptibility of LCs, thereby leading to enhanced sexual transmission of HIV. Notably, a recent study has shown that cervicovaginal levels of LL-37 were associated with increased HIV acquisition in Kenyan sex workers (Levinson et al., 2009), a clinical finding that supports our hypothesis. Thus, HSV-2 can mediate both direct enhancing effects on HIV susceptibility in LCs as well as indirect enhancing effects via LL-37 production as shown here. These results further our understanding of the complex biologic events that occur during the early stages of sexual transmission of HIV.

EXPERIMENTAL PROCEDURES

Reagents

Cells were stimulated with synthetic AMPs (Peptide Institute) for 24 hr at the following concentrations: α defensin-5 (50 μg/ml), β defensin-1 (50 μg/ml), β defensin-2 (50 μg/ml), β defensin-3 (5 μg/ml), β defensin-4 (50 μg/ml), and LL-37 (50 μg/ml). Recombinant human (rh) TNF-α (5 μg/ml, R&D Systems) was used as a positive control in some experiments. Anti-TNF-α neutralizing mAbs (clone; MABTNF-A5) were purchased from BD PharMingen and used at a final concentration of 1 μg/ml.

Cell Preparation

NHEKs were purchased from Kurabo and cultured with EpiLife supplemented with insulin (10 μg/ml), rhEGF (epidermal growth factor, 0.1 ng/ml), hydrocortisone (0.5 μg/ml), gentamicin (50 μg/ml), amphotericin B (50 ng/ml), and bovine pituitary extract (0.4% V/V) (EpiLife-KG2 medium, all from Kurabo) in a humidified atmosphere with 5% CO2 at 37°C.

mLCs and mDCs were cultured from adult plastic-adherent PBMCs as described previously (Kawamura et al., 2001). Briefly, monocytes were isolated by depletion of magnetically labeled nonmonocytes (Monocyte Isolation Kit II, Miltenyi Biotec) from plastic-adherent PBMCs obtained from healthy blood donors. Monocytes were cultured in RPMI 1640 (GIBCO BRL) supplemented with 10% heat-inactivated FBS (Cell Culture Technologies), 100 U/ml penicillin (GIBCO BRL), 100 μg/ml streptomycin (GIBCO BRL), 2 mM L-glutamine (GIBCO BRL) (complete medium) supplemented with 1,000 U/ml rhGM-CSF (R&D Systems), 1,000 U/ml rhIL-4 (R&D Systems), and with mLCs or without mDCs 10 ng/ml human platelet-derived TGF-β1 (R&D Systems) for 7 days. Since we have previously found the expression levels of E-cadherin$^+$ cells and langerin$^+$ cells in mLCs to be approximately 90% and 35%, respectively (Kawamura et al., 2001), cell sorting was performed at day 7 to isolate highly purified langerin-positive mLCs followed by staining with anti-langerin mAb (Immunotech), as previously described (Ogawa et al., 2009). Alternatively, mLCs were identified by gating langerin-positive cells in flow cytometric analyses.

HSV-2 Exposure of Cells In Vitro and Skin Explants Ex Vivo

Purified, pelleted, and titered HSV-2 G strain (stock at 10^8 PFU/ml) was purchased from Advanced Biotechnologies. HSV-2 strain 186 (stock at 1.5×10^7 PFU/ml) was a gift from Yukihiro Nishiyama (Nagoya University Graduate School of Medicine, Nagoya, Japan). A total of 2×10^5 mLCs or mDCs, or 5×10^6 NHEK, were cultured with different concentrations of HSV-2 (10^{4-6} PFU) at 37°C, and then washed three times. In some experiments using the supernatants from NHEKs treated by HSV-2, culture supernatants

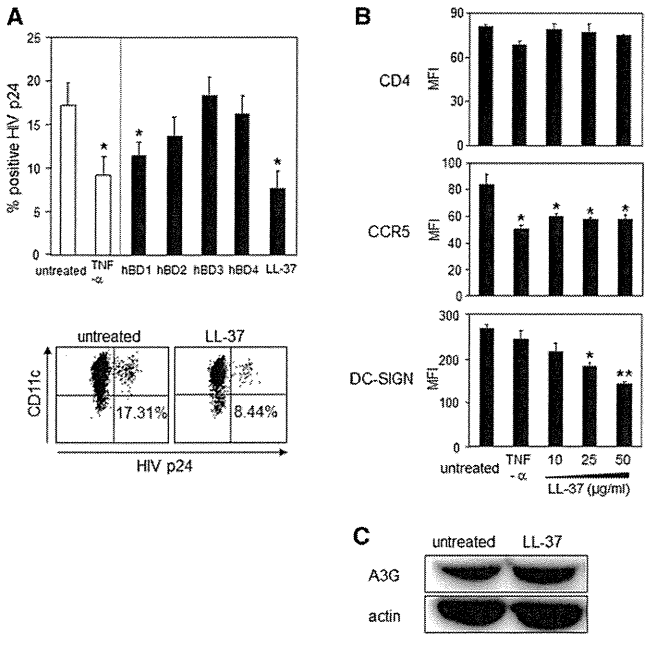

Figure 6. LL-37 Decreases HIV Susceptibility in mDCs

(A) mDCs were stimulated with the indicated AMPs or rhTNF-α 24 hr prior to HIV exposure. To determine HIV infection levels, mDCs were collected 7 days after HIV exposure, and HIV $p24^+$ cells were assessed in $CD11c^+$ mDCs. Representative flow cytometric analyses are shown.

(B) mDCs were stimulated with TNF-α or LL-37 at the indicated concentrations for 24 hr. The expression of CD4, CCR5, and DC-SIGN was assessed by flow cytometry.

(C) The expression of A3G was determined by western blot analysis. Results are shown as means ± SD (n = 3) (*$p < 0.05$; **$p < 0.01$). All data shown represent at least two separate experiments.

containing HSV-2 were filtered by PALL Acrodisc 32 mm Syringe Filter with 0.1 μm Supor Membrane to remove viruses. For control infection, the same batch of virus was inactivated at 56°C for 10 min and the same volume as the active virus was added to cells. For exposure of epithelial tissue explants, 50 μl droplets containing different concentrations of HSV-2 were placed on the inside surfaces of sterile plastic culture dish covers. Explants were draped over droplets with the basal epithelial cell surface facing downward. Virus and explants were incubated together in this manner at 37°C in a humidified 5% CO_2 environment for 1 hr, and then washed three times with cold PBS.

HIV Infection of Cells In Vitro and Skin Explants Ex Vivo

Purified, pelleted, and titered HIV-1Ba-L, an R5 HIV laboratory isolate (stock at $TCID_{50}$ of $10^{7.17}$/ml and 1.8×10^{10} virus particles/ml), was purchased from Advanced Biotechnologies. Molecular clones R5 HIV primary isolates (JR-FL and AD8) were prepared as described previously (Koyanagi et al., 1997; Theodore et al., 1996). Briefly, 293T cells were transfected with 30 μg of HIV-1 proviral DNA. One day after transfection, the medium was replaced with fresh RPMI 1640 medium supplemented with 10% FCS, and then 2 days later, the viruses were recovered, filtered through a membrane (pore size, 0.22 mm), and assayed for HIV-1 p24 gag content by ELISA. The titer of each virus stock was determined by endpoint titer determination of 3-fold limiting dilution in triplicate on PHA-activated PBMC from a single donor. Aliquots of the viral stocks ($TCID_{50}$ of 9,004,929/ml; JR-FL and 7,746,147/ml; AD8) were stored at minus 80°C until use. For some experiments, 2×10^5 mLCs and mDCs were preincubated with various agonists, inhibitors, HSV-2, or the supernatants from NHEKs treated by HSV-2, and then HIV-1Ba-L at a 1/100 final dilution or R5 HIV primary isolates (JR-FL and AD8) at $TCID_{50}$ of 10^5/ml was added for 2 hr at 37°C, as described previously (Kawamura et al., 2001). After incubation, cells were harvested, washed three times in washing medium (HBSS containing 10% heat-inactivated FBS), resuspended in complete medium supplemented with GM-CSF and IL-4, and cultured for 7 additional days at the same cellular concentration. HIV-infected cells were assessed by HIV p24 intracellular staining. Because the variability in the infection levels was most likely due to the *CCR5* heterogeneity in the donors, HIV infection levels with mLCs and mDCs obtained from different donors were not directly compared. Instead, HIV infection levels were expressed as a normalized percent of the positive cells for HIV p24 by using a calculated fold difference as compared with the mean percent of the positive cells for HIV p24 in untreated cells (Figure 3A). In some experiments, 2×10^4 HIV-infected mLCs or mDCs were cocultured with 2×10^6 allogeneic $CD4^+$ T cells for 12 days, and supernatants were harvested every third day and examined for HIV p24 protein content by ELISA (ZeptoMetrix) according to the manufacturer's instructions.

Epithelial sheets were obtained from suction blister roofs from HIV-negative healthy donors. For infection of epithelial tissue explants, 50 μl droplets containing HIV-1Ba-L at a 1/100 final dilution were placed on the inside surfaces of sterile plastic culture dish covers, as described previously (Kawamura et al., 2000). Explants were draped over droplets with the basal epithelial cell surface facing downward. Virus and explants were incubated together in this manner at 37°C in a humidified 5% CO_2 environment for 2 hr. Explants were washed in three separate wells in 6-well plates containing sterile PBS and then floated with the basal epithelial cell sides down in 12-well plates containing 2 ml of complete medium, without exogenous stimulants or cytokines. The emigrating cells from the epidermal sheets were collected 3 days after the HIV exposure. In some experiments, epidermal cell suspensions were prepared by limited trypsinization of epidermal sheets, as described previously (Miller et al., 2011a).

Pseudotyped Virus Infection and Luciferase Assay

To prepare pseudotyped viruses with Env from either HIV-1 (IIIB, JR-FL, or VSV), 293 T cells were cotransfected with the Env expression plasmid DNA, pLET, pJRFLenv, or pMD.G, respectively, and with pNLLuc (an Env-defective HIV-1NL4-3 carrying the luciferase gene) as described previously (Sato et al., 2008). The culture supernatants were harvested and then filtrated to produce virus solutions at 48 hr posttransfection. To measure the infectivity of Env-pseudotyped virus, mLCs were incubated with JR-FL Env- or IIIB Env-pseudotyped virus, containing 20 ng of p24CA, or VSV envelope glycoprotein-pseudotyped virus, containing 0.5 ng of p24CA, for 72 hr. The Picagene luciferase assay kit (Toyo Ink) was used to perform luciferase assays, following the manufacturer's protocols. Activity was measured with a 1420 ARVOSX multilabel counter (Perkin Elmer) and normalized to the protein content of each lysate, measured with a Coomassie (Bradford) protein assay kit (Pierce).

Flow Cytometry

Single-cell suspensions were stained using the following anti-human mAb: anti-CD83 (BD Biosciences-PharMingen), anti-CD86 (BD Biosciences-PharMingen), anti-CD4 (Beckman Coulter), anti-CCR5 (R&D), anti-DC-sign (R&D), anti-CCR7 (R&D) directly conjugated to FITC, anti-langerin (Immunotech) directly conjugated to PE, and anti-CD11c (Becton Dickinson) directly conjugated to allophycocyanin. Cells were incubated with Abs for 30 min at 4°C and then washed three times in staining buffer and examined by FACScaliber using propidium iodide (Sigma) to exclude the dead cells in the surface staining.

To specifically identify HIV- or HSV-infected cells on a single-cell level, HIV p24 or HSV gD intracellular staining was performed, respectively. Epidermal LCs, mLCs, and mDCs were collected at the indicated days after HIV exposure and then washed three times in staining buffer, and then incubated with 10 μg/ml allophycocyanin-conjugated mouse anti-human CD11c mAb, and with mLCs or without mDCs PE-conjugated mouse anti-human langerin mAb and for 30 min at 4°C. Cells were then washed three times in staining buffer and fixed and permeabilized with Cytofix/Cytoperm reagents (BD Biosciences-PharMingen) for 20 min at 4°C. Cells were then washed three times in Perm-Wash (BD Biosciences-PharMingen), incubated with FITC- or PE-conjugated mouse anti-HIV p24 mAb (Beckman Coulter) and/or FITC-conjugated mouse anti-HSV gD mAb (Argene) diluted for 30 min at 4°C, and washed three times in Perm-Wash, with the quantified numbers of HIV- or HSV-infected cells determined by FACScaliber.

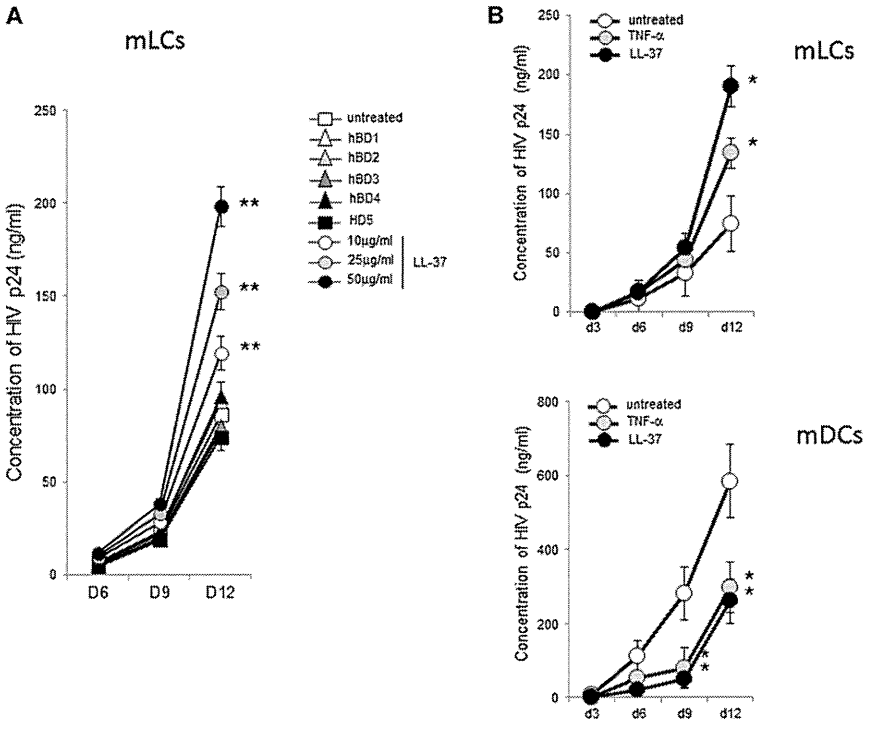

Figure 7. LL-37 Enhances HIV Transmission from mLCs to T Cells

mLCs (A) or mLCs and mDCs isolated from the same donor (B) were stimulated with the indicated AMPs or rhTNF-α 24 hr prior to HIV exposure. HIV-infected mLCs or mDCs were cocultured with allogeneic $CD4^+$ T cells, and p24 protein levels in culture supernatants were assessed by ELISA on the indicated days. Results are shown as means plus or minus SD (n = 3). *$p < 0.05$; **$p < 0.01$. All data shown represent at least two separate experiments.

RNA Interference Using siRNA

The delivery of siRNA into NHEKs was performed by DharmaFECT 3 siRNA Transfection Reagent (Dharmacon). Cells were transfected with siRNAs at a final concentration of 50 nM. The siRNAs used in this study were ON-TARGETplus nontargeting pool (Dharmacon #D 001810–10) for control siRNA and ON-TARGETplus SMARTpool siRNA Human CAMP (Dharmacon #L-019790–00) for LL-37 siRNA.

Real-Time Quantitative RT-PCR Analysis

Relative mRNA expression was determined by real-time PCR using an ABI PRISM 5500 Sequence Detection System (Applied Biosystems) with SYBR Green I dye (QIAGEN) according to the manufacturer's instructions. Total RNA was isolated using TRIzol (Invitrogen Life Technologies), and cDNA was synthesized using the SuperScript system (Invitrogen Life Technologies). Primers corresponding to human α defensin-5, defensin-6, human β defensin-1, β defensin-2, β defensin-3, β defensin-4, LL-37, and GAPDH were designed by Takara Bio, Inc. Cycle threshold numbers (Ct) were derived from the exponential phase of the PCR amplification. Fold differences in the expression of gene x in the cell populations y and z were derived by 2k, where k = (Ctx − CtG3PDH)y − (Ctx − CtG3PDH)z.

ELISA

NHEKs were exposed to live HSV-2 (10^6 PFU) or heat-inactivated HSV-2 for 1 hr, and then washed three times. Following culture in medium for the indicated days, the culture supernatants were collected after centrifugation and stored at −80°C for LL-37 and TNF-α measurement. The concentration of human LL-37 (Hycult biotechnology) and TNF-α (R&D Systems) in the culture supernatants was measured by ELISA. For measurement of HIV p24 protein levels, supernatants were collected, inactivated with Triton X-100 (Sigma-Aldrich; 2% final concentration), and kept frozen until measurements of HIV p24 protein levels were performed by ELISA (ZeptoMetrix).

Western Blot Analysis

Proteins of the cells were extracted using 15 min incubation in complete lysis buffer containing a protease inhibitor. Equal amounts of protein were separated by SDS-PAGE and transferred onto a transfer membrane (Daiichikagaku). Western blot was performed in order to detect hCAP18 (2.0 μg/ml, Abcam), KLK5 (2.0 μg/ml, R&D Systems), LL-37 (2.0 μg/ml, Santa Cruz), A3G (2.5 μg/ml, Abcam), and SAMHD1 (2.0 μg/ml, Abcam). Blots were incubated with the HRP-linked secondary antibody. Analyses were performed using the HRP western blot detection system (Pierce), and band intensities were calculated using ImageJ software.

Statistical Analyses

Significant differences between experimental groups were analyzed by Student's t test (one-tailed). p values less than 0.05 were considered significant.

Study Approval

The Institutional Review Board of the University Hospital (University of Yamanashi, Yamanashi, Japan) approved the acquisition of human tissues, and informed consent was obtained from all skin donors.

SUPPLEMENTAL INFORMATION

Supplemental Information includes five figures and can be found with this article at http://dx.doi.org/10.1016/j.chom.2012.12.002.

ACKNOWLEDGMENTS

We would like to thank Kazutoshi Harada and Naotaka Shibagaki for their helpful discussions; Miyuki Ogino and Naoko Misawa for technical assistance; and Takashi Fujita, Keizo Tomonaga, and Klaus Strebel for providing reagents. These studies were supported in part by a grant from the Ministry of Education and Science of the Japanese Government. Y.O. performed experiments and analyzed data. T.K. directed and performed experiments, analyzed data, and wrote the manuscript. T.M. and R.A. performed experiments and analyzed data. P.G. and A.Y. performed experiments. K.M. contributed analytical tools. K.Y. and Y.K. codirected experiments. A.B. codirected experiments and wrote the manuscript. S.S. codirected experiments.

Received: June 28, 2012
Revised: September 18, 2012
Accepted: December 12, 2012
Published: January 16, 2013

REFERENCES

Auvert, B., Taljaard, D., Lagarde, E., Sobngwi-Tambekou, J., Sitta, R., and Puren, A. (2005). Randomized, controlled intervention trial of male circumcision for reduction of HIV infection risk: the ANRS 1265 Trial. PLoS Med. *2*, e298. http://dx.doi.org/10.1371/journal.pmed.0020298.

Bailey, R.C., Moses, S., Parker, C.B., Agot, K., Maclean, I., Krieger, J.N., Williams, C.F., Campbell, R.T., and Ndinya-Achola, J.O. (2007). Male circumcision for HIV prevention in young men in Kisumu, Kenya: a randomised controlled trial. Lancet *369*, 643–656.

Bergman, P., Walter-Jallow, L., Broliden, K., Agerberth, B., and Söderlund, J. (2007). The antimicrobial peptide LL-37 inhibits HIV-1 replication. Curr. HIV Res. *5*, 410–415.

Cameron, D.W., Simonsen, J.N., D'Costa, L.J., Ronald, A.R., Maitha, G.M., Gakinya, M.N., Cheang, M., Ndinya-Achola, J.O., Piot, P., Brunham, R.C., et al. (1989). Female to male transmission of human immunodeficiency virus type 1: risk factors for seroconversion in men. Lancet *2*, 403–407.

Cunningham, A.L., Turner, R.R., Miller, A.C., Para, M.F., and Merigan, T.C. (1985). Evolution of recurrent herpes simplex lesions. An immunohistologic study. J. Clin. Invest. *75*, 226–233.

de Jong, M.A., de Witte, L., Oudhoff, M.J., Gringhuis, S.I., Gallay, P., and Geijtenbeek, T.B. (2008). TNF-alpha and TLR agonists increase susceptibility to HIV-1 transmission by human Langerhans cells ex vivo. J. Clin. Invest. *118*, 3440–3452.

de Jong, M.A., de Witte, L., Taylor, M.E., and Geijtenbeek, T.B. (2010). Herpes simplex virus type 2 enhances HIV-1 susceptibility by affecting Langerhans cell function. J. Immunol. *185*, 1633–1641.

de Witte, L., Nabatov, A., Pion, M., Fluitsma, D., de Jong, M.A., de Gruijl, T., Piguet, V., van Kooyk, Y., and Geijtenbeek, T.B. (2007). Langerin is a natural barrier to HIV-1 transmission by Langerhans cells. Nat. Med. *13*, 367–371.

Fahrbach, K.M., Barry, S.M., Anderson, M.R., and Hope, T.J. (2010). Enhanced cellular responses and environmental sampling within inner foreskin explants: implications for the foreskin's role in HIV transmission. Mucosal Immunol. *3*, 410–418.

Fleming, D.T., and Wasserheit, J.N. (1999). From epidemiological synergy to public health policy and practice: the contribution of other sexually transmitted diseases to sexual transmission of HIV infection. Sex. Transm. Infect. *75*, 3–17.

Galvin, S.R., and Cohen, M.S. (2004). The role of sexually transmitted diseases in HIV transmission. Nat. Rev. Microbiol. *2*, 33–42.

Ganor, Y., Zhou, Z., Tudor, D., Schmitt, A., Vacher-Lavenu, M.C., Gibault, L., Thiounn, N., Tomasini, J., Wolf, J.P., and Bomsel, M. (2010). Within 1 h, HIV-1 uses viral synapses to enter efficiently the inner, but not outer, foreskin mucosa and engages Langerhans-T cell conjugates. Mucosal Immunol. *3*, 506–522.

Gray, R.H., Kigozi, G., Serwadda, D., Makumbi, F., Watya, S., Nalugoda, F., Kiwanuka, N., Moulton, L.H., Chaudhary, M.A., Chen, M.Z., et al. (2007). Male circumcision for HIV prevention in men in Rakai, Uganda: a randomised trial. Lancet *369*, 657–666.

Gringhuis, S.I., van der Vlist, M., van den Berg, L.M., den Dunnen, J., Litjens, M., and Geijtenbeek, T.B. (2010). HIV-1 exploits innate signaling by TLR8 and DC-SIGN for productive infection of dendritic cells. Nat. Immunol. *11*, 419–426.

Grivel, J.C., Shattock, R.J., and Margolis, L.B. (2011). Selective transmission of R5 HIV-1 variants: where is the gatekeeper? J. Transl. Med. *9(Suppl 1)*, S6.

Haase, A.T. (2010). Targeting early infection to prevent HIV-1 mucosal transmission. Nature *464*, 217–223.

Hrecka, K., Hao, C., Gierszewska, M., Swanson, S.K., Kesik-Brodacka, M., Srivastava, S., Florens, L., Washburn, M.P., and Skowronski, J. (2011). Vpx relieves inhibition of HIV-1 infection of macrophages mediated by the SAMHD1 protein. Nature *474*, 658–661.

Hu, J., Gardner, M.B., and Miller, C.J. (2000). Simian immunodeficiency virus rapidly penetrates the cervicovaginal mucosa after intravaginal inoculation and infects intraepithelial dendritic cells. J. Virol. *74*, 6087–6095.

Kawamura, T., Cohen, S.S., Borris, D.L., Aquilino, E.A., Glushakova, S., Margolis, L.B., Orenstein, J.M., Offord, R.E., Neurath, A.R., and Blauvelt, A. (2000). Candidate microbicides block HIV-1 infection of human immature Langerhans cells within epithelial tissue explants. J. Exp. Med. *192*, 1491–1500.

Kawamura, T., Qualbani, M., Thomas, E.K., Orenstein, J.M., and Blauvelt, A. (2001). Low levels of productive HIV infection in Langerhans cell-like dendritic cells differentiated in the presence of TGF-beta1 and increased viral replication with CD40 ligand-induced maturation. Eur. J. Immunol. *31*, 360–368.

Kawamura, T., Gulden, F.O., Sugaya, M., McNamara, D.T., Borris, D.L., Lederman, M.M., Orenstein, J.M., Zimmerman, P.A., and Blauvelt, A. (2003). R5 HIV productively infects Langerhans cells, and infection levels are regulated by compound CCR5 polymorphisms. Proc. Natl. Acad. Sci. USA *100*, 8401–8406.

Kawamura, T., Kurtz, S.E., Blauvelt, A., and Shimada, S. (2005). The role of Langerhans cells in the sexual transmission of HIV. J. Dermatol. Sci. *40*, 147–155.

Kawamura, T., Koyanagi, Y., Nakamura, Y., Ogawa, Y., Yamashita, A., Iwamoto, T., Ito, M., Blauvelt, A., and Shimada, S. (2008). Significant virus replication in Langerhans cells following application of HIV to abraded skin: relevance to occupational transmission of HIV. J. Immunol. *180*, 3297–3304.

Klotman, M.E., and Chang, T.L. (2006). Defensins in innate antiviral immunity. Nat. Rev. Immunol. *6*, 447–456.

Klotman, M.E., Rapista, A., Teleshova, N., Micsenyi, A., Jarvis, G.A., Lu, W., Porter, E., and Chang, T.L. (2008). Neisseria gonorrhoeae-induced human defensins 5 and 6 increase HIV infectivity: role in enhanced transmission. J. Immunol. *180*, 6176–6185.

Koyanagi, Y., Tanaka, Y., Kira, J., Ito, M., Hioki, K., Misawa, N., Kawano, Y., Yamasaki, K., Tanaka, R., Suzuki, Y., et al. (1997). Primary human immunodeficiency virus type 1 viremia and central nervous system invasion in a novel hu-PBL-immunodeficient mouse strain. J. Virol. *71*, 2417–2424.

Laguette, N., Sobhian, B., Casartelli, N., Ringeard, M., Chable-Bessia, C., Ségéral, E., Yatim, A., Emiliani, S., Schwartz, O., and Benkirane, M. (2011). SAMHD1 is the dendritic- and myeloid-cell-specific HIV-1 restriction factor counteracted by Vpx. Nature *474*, 654–657.

Lederman, M.M., Veazey, R.S., Offord, R., Mosier, D.E., Dufour, J., Mefford, M., Piatak, M., Jr., Lifson, J.D., Salkowitz, J.R., Rodriguez, B., et al. (2004). Prevention of vaginal SHIV transmission in rhesus macaques through inhibition of CCR5. Science *306*, 485–487.

Lederman, M.M., Offord, R.E., and Hartley, O. (2006). Microbicides and other topical strategies to prevent vaginal transmission of HIV. Nat. Rev. Immunol. *6*, 371–382.

Levinson, P., Kaul, R., Kimani, J., Ngugi, E., Moses, S., MacDonald, K.S., Broliden, K., and Hirbod, T.; Kibera HIV Study Group. (2009). Levels of innate immune factors in genital fluids: association of alpha defensins and LL-37 with genital infections and increased HIV acquisition. AIDS *23*, 309–317.

Liu, R., Paxton, W.A., Choe, S., Ceradini, D., Martin, S.R., Horuk, R., MacDonald, M.E., Stuhlmann, H., Koup, R.A., and Landau, N.R. (1996). Homozygous defect in HIV-1 coreceptor accounts for resistance of some multiply-exposed individuals to HIV-1 infection. Cell *86*, 367–377.

Miller, C.J., Johnson, S.L., Kwapil, T.R., and Carver, C.S. (2011a). Three studies on self-report scales to detect bipolar disorder. J. Affect. Disord. *128*, 199–210.

Miller, C.J., Rose, A.L., and Waite, T.D. (2011b). Phthalhydrazide chemiluminescence method for determination of hydroxyl radical production: modifications and adaptations for use in natural systems. Anal. Chem. *83*, 261–268.

Morizane, S., Yamasaki, K., Kabigting, F.D., and Gallo, R.L. (2010). Kallikrein expression and cathelicidin processing are independently controlled in keratinocytes by calcium, vitamin D(3), and retinoic acid. J. Invest. Dermatol. *130*, 1297–1306.

Ogawa, Y., Kawamura, T., Kimura, T., Ito, M., Blauvelt, A., and Shimada, S. (2009). Gram-positive bacteria enhance HIV-1 susceptibility in Langerhans cells, but not in dendritic cells, via Toll-like receptor activation. Blood *113*, 5157–5166.

Ong, P.Y., Ohtake, T., Brandt, C., Strickland, I., Boguniewicz, M., Ganz, T., Gallo, R.L., and Leung, D.Y. (2002). Endogenous antimicrobial peptides and skin infections in atopic dermatitis. N. Engl. J. Med. *347*, 1151–1160.

Pion, M., Granelli-Piperno, A., Mangeat, B., Stalder, R., Correa, R., Steinman, R.M., and Piguet, V. (2006). APOBEC3G/3F mediates intrinsic resistance of monocyte-derived dendritic cells to HIV-1 infection. J. Exp. Med. *203*, 2887–2893.

Quiñones-Mateu, M.E., Lederman, M.M., Feng, Z., Chakraborty, B., Weber, J., Rangel, H.R., Marotta, M.L., Mirza, M., Jiang, B., Kiser, P., et al. (2003). Human epithelial beta-defensins 2 and 3 inhibit HIV-1 replication. AIDS *17*, F39–F48.

Reece, J.C., Handley, A.J., Anstee, E.J., Morrison, W.A., Crowe, S.M., and Cameron, P.U. (1998). HIV-1 selection by epidermal dendritic cells during transmission across human skin. J. Exp. Med. *187*, 1623–1631.

Sato, K., Aoki, J., Misawa, N., Daikoku, E., Sano, K., Tanaka, Y., and Koyanagi, Y. (2008). Modulation of human immunodeficiency virus type 1 infectivity through incorporation of tetraspanin proteins. J. Virol. *82*, 1021–1033.

Shattock, R.J., and Moore, J.P. (2003). Inhibiting sexual transmission of HIV-1 infection. Nat. Rev. Microbiol. *1*, 25–34.

Spira, A.I., Marx, P.A., Patterson, B.K., Mahoney, J., Koup, R.A., Wolinsky, S.M., and Ho, D.D. (1996). Cellular targets of infection and route of viral dissemination after an intravaginal inoculation of simian immunodeficiency virus into rhesus macaques. J. Exp. Med. *183*, 215–225.

Sun, L., Finnegan, C.M., Kish-Catalone, T., Blumenthal, R., Garzino-Demo, P., La Terra Maggiore, G.M., Berrone, S., Kleinman, C., Wu, Z., Abdelwahab, S., et al. (2005). Human beta-defensins suppress human immunodeficiency virus infection: potential role in mucosal protection. J. Virol. *79*, 14318–14329.

Theodore, T.S., Englund, G., Buckler-White, A., Buckler, C.E., Martin, M.A., and Peden, K.W. (1996). Construction and characterization of a stable full-length macrophage-tropic HIV type 1 molecular clone that directs the production of high titers of progeny virions. AIDS Res. Hum. Retroviruses *12*, 191–194.

Wald, A., and Link, K. (2002). Risk of human immunodeficiency virus infection in herpes simplex virus type 2-seropositive persons: a meta-analysis. J. Infect. Dis. *185*, 45–52.

Yamasaki, K., Schauber, J., Coda, A., Lin, H., Dorschner, R.A., Schechter, N.M., Bonnart, C., Descargues, P., Hovnanian, A., and Gallo, R.L. (2006). Kallikrein-mediated proteolysis regulates the antimicrobial effects of cathelicidins in skin. FASEB J. *20*, 2068–2080.

Yamasaki, K., Di Nardo, A., Bardan, A., Murakami, M., Ohtake, T., Coda, A., Dorschner, R.A., Bonnart, C., Descargues, P., Hovnanian, A., et al. (2007). Increased serine protease activity and cathelicidin promotes skin inflammation in rosacea. Nat. Med. *13*, 975–980.

Zaitseva, M., Blauvelt, A., Lee, S., Lapham, C.K., Klaus-Kovtun, V., Mostowski, H., Manischewitz, J., and Golding, H. (1997). Expression and function of CCR5 and CXCR4 on human Langerhans cells and macrophages: implications for HIV primary infection. Nat. Med. *3*, 1369–1375.

Zhang, Z.Q., Schuler, T., Cavert, W., Notermans, D.W., Gebhard, K., Henry, K., Havlir, D.V., Günthard, H.F., Wong, J.K., Little, S., et al. (1999). Reversibility of the pathological changes in the follicular dendritic cell network with treatment of HIV-1 infection. Proc. Natl. Acad. Sci. USA *96*, 5169–5172.

Zhou, Z., Barry de Longchamps, N., Schmitt, A., Zerbib, M., Vacher-Lavenu, M.C., Bomsel, M., and Ganor, Y. (2011). HIV-1 efficient entry in inner foreskin is mediated by elevated CCL5/RANTES that recruits T cells and fuels conjugate formation with Langerhans cells. PLoS Pathog. *7*, e1002100. http://dx.doi.org/10.1371/journal.ppat.1002100.

Zhu, T., Mo, H., Wang, N., Nam, D.S., Cao, Y., Koup, R.A., and Ho, D.D. (1993). Genotypic and phenotypic characterization of HIV-1 patients with primary infection. Science *261*, 1179–1181.

Zhu, J., Hladik, F., Woodward, A., Klock, A., Peng, T., Johnston, C., Remington, M., Magaret, A., Koelle, D.M., Wald, A., and Corey, L. (2009). Persistence of HIV-1 receptor-positive cells after HSV-2 reactivation is a potential mechanism for increased HIV-1 acquisition. Nat. Med. *15*, 886–892.

JVI
Journals.ASM.org

Deep-Sequencing Analysis of the Association between the Quasispecies Nature of the Hepatitis C Virus Core Region and Disease Progression

Mika Miura,[a] Shinya Maekawa,[a] Shinichi Takano,[a] Nobutoshi Komatsu,[a] Akihisa Tatsumi,[a] Yukiko Asakawa,[a] Kuniaki Shindo,[a] Fumitake Amemiya,[a] Yasuhiro Nakayama,[a] Taisuke Inoue,[a] Minoru Sakamoto,[a] Atsuya Yamashita,[b] Kohji Moriishi,[b] Nobuyuki Enomoto[a]

First Department of Internal Medicine, Faculty of Medicine, University of Yamanashi, Shimokato, Chuo, Yamanashi, Japan[a]; Department of Microbiology, University of Yamanashi, Shimokato, Chuo, Yamanashi, Japan[b]

Variation of core amino acid (aa) 70 of hepatitis C virus (HCV) has been shown recently to be closely correlated with liver disease progression, suggesting that the core region might be present as a quasispecies during persistent infection and that this quasispecies nature might have an influence on the progression of disease. In our investigation, the subjects were 79 patients infected with HCV genotype 1b (25 with chronic hepatitis [CH], 29 with liver cirrhosis [LC], and 25 with hepatocellular carcinoma [HCC]). Deep sequencing of the HCV core region was carried out on their sera by using a Roche 454 GS Junior pyrosequencer. Based on a plasmid containing a cloned HCV sequence (pCV-J4L6S), the background error rate associated with pyrosequencing, including the PCR procedure, was calculated as 0.092 ± 0.005/base. Deep sequencing of the core region in the clinical samples showed a mixture of "mutant-type" Q/H and "wild-type" R at the core aa 70 position in most cases (71/79 [89.9%]), and the ratio of mutant residues to R in the mixture increased as liver disease advanced to LC and HCC. Meanwhile, phylogenetic analysis of the almost-complete core region revealed that the HCV isolates differed genetically depending on the mutation status at core aa 70. We conclude that the core aa 70 mixture ratio, determined by deep sequencing, reflected the status of liver disease, demonstrating a significant association between core aa 70 and disease progression in CH patients infected with HCV genotype 1b.

Hepatitis C virus (HCV)-related liver disease gradually advances from chronic hepatitis (CH) to liver cirrhosis (LC) and to hepatocellular carcinoma (HCC) over 20 to 30 years (1). However, the rates of disease progression differ: some patients develop HCC over several years, while others show persistently normal alanine aminotransferase (PNALT) levels for decades, and the cause of the difference remains poorly understood.

The involvement of viral and host factors in the progression of liver disease and hepatocarcinogenesis is complex (2). With regard to viral factors, the relationship between the viral core region and disease progression in HCV genotype 1b infection has attracted clinical attention. Specifically, it has been reported that the core amino acid (aa) 70 residue, identified as a variable related to the outcome of interferon (IFN) therapy (3), is closely associated with the progression of hepatitis and hepatocarcinogenesis in Japan and North America (4–7). Those previous studies and our own have reported that core aa 70 variation is strongly linked to carcinogenesis and that substitutions in the core aa 70 region aggravate hepatitis and heighten the risk of hepatocarcinogenesis during the clinical course, corroborating the relationship between the status of the core region and disease progression (8, 9).

With regard to host factors, a genomewide association study (GWAS) has recently shown that single nucleotide polymorphisms (SNPs) around the interleukin 28B (IL28B) gene (rs12979860 and rs8099917), encoding the type III IFN IFN-λ3, are strongly correlated with the outcomes of therapy with pegylated IFN-α plus ribavirin for chronic hepatitis C (CH-C) (10–13). Interestingly, in contrast to the core region, consensus has not been reached as to the relationship between disease progression and the IL28B SNP, which is associated with IFN resistance (14–17). Previously, we reported that there was no correlation between the onset of HCC and the IL28B SNP (9). However, it was reported that the IL28B rs8099917 TG/GG allele was markedly correlated with the presence of Q (glutamine) or H (histidine) instead of the R (arginine) residue at core aa 70, while the IL28B rs8099917 TT allele was correlated with core aa 70R (8). Moreover, the core amino acid R70Q/H change occurs more often in patients with IL28B rs8099917 TG/GG than in those with IL28B rs8099917 TT (9). In this manner, the contributions of the core aa 70 residue and the IL28B SNP, which were found to be IFN sensitivity factors, to the progression of liver disease have gradually been elucidated.

HCV exists in a host as a swarm of variants, known as a "quasispecies," and this quasispecies nature has been considered to play a critical role in pathogenesis (18). However, detailed analysis has been technically difficult, and the clinical significance has not been clarified in detail thus far. Considering the observation of core aa 70 gene changes over time, it is assumed that a variety of core aa 70 isolates may exist as a quasispecies, and this could be related to pathogenesis as described above.

Recently, deep-sequencing technology has advanced rapidly and has enabled us to analyze viral quasispecies in association with the status of the disease (19–22). In this study, we investigated how the quasispecies of the HCV core gene, either at the hot spot of the core aa 70 residue or in the almost-entire core gene, is created and is involved in disease progression in patients with CH-C.

Received 28 March 2013 Accepted 7 August 2013
Published ahead of print 14 August 2013
Address correspondence to Shinya Maekawa, maekawa@yamanashi.ac.jp.
Supplemental material for this article may be found at http://dx.doi.org/10.1128/JVI.00826-13.

doi:10.1128/JVI.00826-13

TABLE 1 Patient characteristics classified by disease progression

Characteristic[a]	Value for patients with:			P
	CH (n = 25)	LC (n = 29)	HCC (n = 25)	
No. male/female	14/11	10/19	12/13	0.278
Age (yr) (mean ± SD)	63.4 ± 14.6	66.5 ± 9.2	68.4 ± 8.2	0.539
Platelets (10^{-4}/mm^3) (mean ± SD)	16.1 ± 4.7	9.8 ± 3.9	11.1 ± 5.1	<0.001
Albumin (g/dl) (mean ± SD)	4.4 ± 0.3	3.9 ± 0.6	3.5 ± 0.5	<0.001
γ-GTP (IU/liter) (median [range])	53.5 (12–230)	38.0 (12–108)	40.8 (15–110)	0.845
T. chol. (mg/dl) (mean ± SD)	161 ± 28	148 ± 30	140 ± 28	0.053
HCV RNA (kIU/ml) (median [range])	7,047 (501–19,953)	5,369 (126–25,119)	8,421 (110–25,119)	0.288
Alpha-fetoprotein (ng/ml) (median [range])	5.0 (1.1–16.5)	32.2 (1.0–252.6)	614.8 (1.9–13,418)	<0.001
AST (IU/liter) (mean ± SD)	42.4 ± 17.8	51.1 ± 23.5	59.1 ± 28.2	0.046
ALT (IU/liter) (mean ± SD)	46.6 ± 23.1	43.9 ± 29.3	60.7 ± 52.7	0.263
No. with R/(Q/H) at core aa 70[b]	19/6	12/17	8/17	0.005
No. with L/(M/C) at core aa 91[b]	17/8	19/10	15/10	0.834
No. of ISDR mutations (median [range])[b]	0.8 (0–6)	1.2 (0–7)	0.9 (0–8)	0.799
No. of IRRDR mutations (median [range])[b]	4.9 (1–10)	4.7 (2–9)	5.2 (1–12)	0.962
No. with TT/non-TT at IL28B SNP (rs8099917)	18/7	17/12	14/11	0.458
No. without/with a history of interferon therapy	14/11	16/13	15/10	0.933

[a] T. chol., total cholesterol; AST, aspartate transaminase; ALT, alanine aminotransferase.
[b] Core aa 70, core aa 91, the interferon sensitivity-determining region (ISDR), and the interferon-ribavirin resistance-determining region (IRRDR) were dominant viral sequences determined by direct sequencing.

PATIENTS AND METHODS

Patients. The subjects were 79 patients persistently infected with HCV genotype 1b who were followed up at Yamanashi University Hospital. The patients all fulfilled the following criteria: (i) they were negative for hepatitis B surface antigen; (ii) they had no other forms of hepatitis, such as primary biliary cirrhosis, autoimmune liver disease, or alcoholic liver disease; (iii) they were free of coinfection with human immunodeficiency virus; and (iv) signed consent was obtained for the study protocol. The study protocol had been approved by the Human Ethics Review Committee of Yamanashi University Hospital and conformed to the ethical guidelines of the Declaration of Helsinki.

The breakdown was as follows: 25 patients with CH, 29 with LC, and 25 with HCC. The patients' clinical backgrounds, including histories of interferon-based antiviral therapy, are shown in Table 1. Deep-sequencing analysis was performed using serum samples taken at the most recent visit from patients with chronic hepatitis or liver cirrhosis and at the first diagnosis of HCC from patients with HCC. A direct-sequencing method, which determines the dominant viral sequence, was performed as described previously (9) to determine the dominant viral sequences of the core region, the interferon sensitivity-determining region (ISDR), and the interferon-ribavirin resistance-determining region (IRRDR) from the serum of each patient.

Deep sequencing. Deep sequencing of the viral core region was performed for each of 79 patients. Briefly, RNA was extracted from the stored sera of these patients and was reverse transcribed to cDNA. Then two-step nested PCR was carried out with primers specific for the core region of the HCV genome (23). The primers for the second-round PCR had barcodes attached, were 10 nucleotides (nt) long, and differed for each sample, so that PCR products from each sample were identifiable (see Table S1 in the supplemental material). After the band densities of the PCR products were quantified using a Bioanalyzer (Agilent Technologies, Palo Alto, CA), the concentrations of the samples were adjusted to a common value, and pooled samples were prepared. Libraries were then subjected to emulsion PCR, the enriched DNA beads loaded onto a picotiter plate, and pyrosequencing carried out with a Roche GS Junior/454 sequencing system using titanium chemistry (Roche, Branford, CT). In order to determine the error rate of the procedure, deep sequencing was carried out under similar conditions with a plasmid containing a cloned HCV sequence (pCV-J4L6S) (24). Amplicon Variant Analyzer software, version 2.5p1 (Roche), was used for analysis.

A dominant sequence of the core region for each patient was deposited in GenBank. Although the study amplified 499 nucleotides, from the 25th to the 523rd nucleotide of the core region, by PCR (Fig. 1), information for only 459 of the 499 nucleotides was uploaded for each patient, since some minor PCR amplicons obtained by deep sequencing did not include the full 499 nucleotides.

Phylogenetic tree analysis. Phylogenetic trees were constructed from the sequences by using the neighbor-joining method with BioEdit and MEGA5.05, and bootstrapping was performed with 1,000 replicates (25). In constructing phylogenetic trees, the three bases of the core codon 70 were removed in the analysis of all trees, since the mutation rate of other parts of the core region is known to be rather low, and it was possible that the influence of the core aa 70 mutations might be overestimated in the phylogenetic trees. In addition, using genetic distance data obtained from the phylogenetic analysis, the genetic distances between every two HCVs with core aa 70R, between every two HCVs with a residue other than R at core aa 70 (core aa 70non-R), and between every two HCVs with different residues at core aa 70 (one HCV with R and one with a non-R residue) were also compared statistically in order to reveal the genetic associations among those HCV core subgroups.

Statistical analysis. Statistical differences in the parameters, including all available patients' demographic, biochemical, hematological, virological, and SNP data in the three groups (CH, LC, and HCC), were determined using the Kruskal-Wallis test. The Mann-Whitney U test was used for statistical differences in numerical variables between two groups. Trends for categorical data

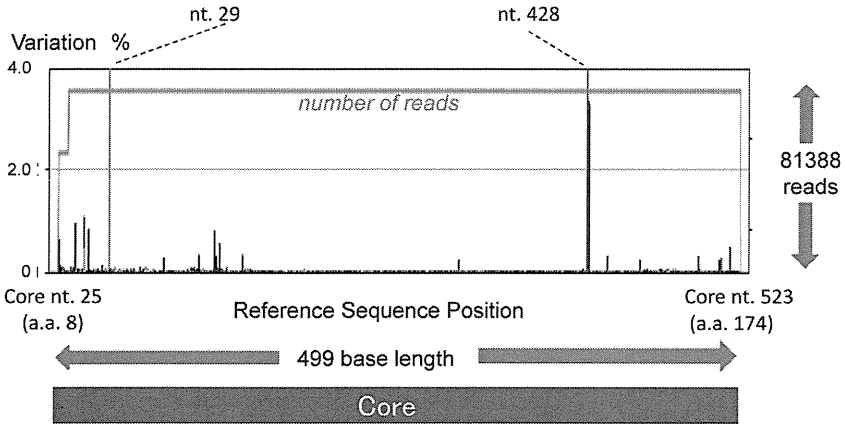

FIG 1 The core region of pCV-J4L6S (genotype 1b) from the 25th to the 523rd nucleotide, and from the 9th to the 174th codon, was subjected to deep sequencing, and the background error rate of pyrosequencing was calculated. In order to show rare background errors, those errors with low percentages are magnified.

were evaluated using the Cochran-Armitage trend test. All *P* values of <0.05 by the two-tailed test were considered significant in comparisons of genetic distances.

Nucleotide sequence accession numbers. The dominant sequences of the core regions from the patient samples have been deposited in GenBank under accession numbers AB822372.1 to AB822459.1.

RESULTS

Calculation of background errors in deep sequencing. First, the background error rate of pyrosequencing was calculated with a plasmid containing a cloned HCV sequence (pCV-J4L6S). Figure 1 shows the results of deep sequencing from the 25th to the 523rd nucleotide of the core region (499 nt) in pCV-J4L6S. Among 81,388 reads, each 499 nt long, the maximum error rate was 99.14% at the 428th base, and the next highest error rate was 64.17% at the 29th base. A six-C homopolymer region ending at the 428th base was read as a five-C homopolymer and a five-A homopolymer region ending at the 29th base was read as a four-A homopolymer in most of the obtained sequences; these homopolymer sequences are a weak point of pyrosequencing (26, 27).

A base appearing six times consecutively was the longest sequence of identical repeated nucleotides and was found only at the 428th nt position in the core region of pCV-J4L6S. Five consecutive bases were found at two sites (the 336th and 436th nt) in addition to the 29th nt position, but this error (i.e., the miscounting of homopolymer length) occurred only at the 29th base closest to the end of the sequence. Excluding the 428th and 29th nt positions, the error rate was ~1% or lower, as shown in Fig. 1. There was no single nucleotide error in the codons for aa 70 and aa 91in the repeated control experiments. From repeated deep sequencing of the plasmid, the overall nucleotide error rate was calculated as 0.092 ± 0.005 (mean ± standard deviation [SD])/base. Based on this analysis, a mixture of bases detectable above the background error of 0.102% (mean background error rate + 2 SDs) was defined as a real mixture.

Baseline characteristics. The baseline characteristics of the 79 patients are shown in Table 1. The values for viral factors core aa 70 and aa 91, NS5A-ISDR, and NS5A-IRRDR are the results of the direct-sequencing study. As shown in Table 1, the results for the variables platelets, albumin, alpha-fetoprotein, and core aa 70 differed significantly according to disease progression. On the other hand, no difference was observed in core aa 91 and IL28B SNP (rs8099917) according to disease progression.

Quasispecies nature of core amino acid 70 and disease progression. Deep sequencing of the core region was carried out with a variety of clinical samples. Simultaneous analysis was carried out using the barcoded primers, and approximately 950 reads were obtained per sample (Table 2). When the analysis was focused on core aa 70, the proportion of non-R (Q/H) sequences increased as disease severity advanced from CH to LC to HCC, as shown in Fig. 2A and Table 3 ($P = 0.018$). When a mixture of 0.102% or more was defined as a real mixture, deep sequencing showed the presence of a mixture at core aa 70 in 71 of the 79 patients (89.9%).

The relationship between disease progression and the occurrence of a quasispecies was also analyzed at the codon for core aa 91, which has also been reported to be associated with the outcomes of IFN therapy and the occurrence of HCC. As with core aa 70, a quasispecies was recognized at this site, and mixtures were observed in most patients. However, in contrast to the core aa 70 codon, there was no clear relationship with disease progression (Fig. 2B and Table 3).

Figure 2C and D show the correlation between mixtures in the core aa 70 and 91 regions and IL28B SNPs. As shown in Fig. 2C and Table 4, the proportion of mutations in the core aa 70 codon was highly dependent on the IL28B SNP (*P*, <0.005 [Table 4]). Such a relationship was also found between the proportion of mutations in core aa 91 and IL28B SNPs (Fig. 2D and Table 4), although its significance was rather weaker (*P*, 0.010).

TABLE 2 Amplicon read numbers obtained by deep sequencing of samples from 79 patients

Group	No. of patients	Total no. of reads	Avg no. of reads ± SD (range)/sample
CH	25	22,365	894.6 ± 222.8 (367–1,486)
LC	29	28,537	982.5 ± 258.1 (660–1,528)
HCC	25	24,284	971.4 ± 242.5 (405–1,749)
Total	79	75,186	951.7 ± 240.9 (367–1,749)

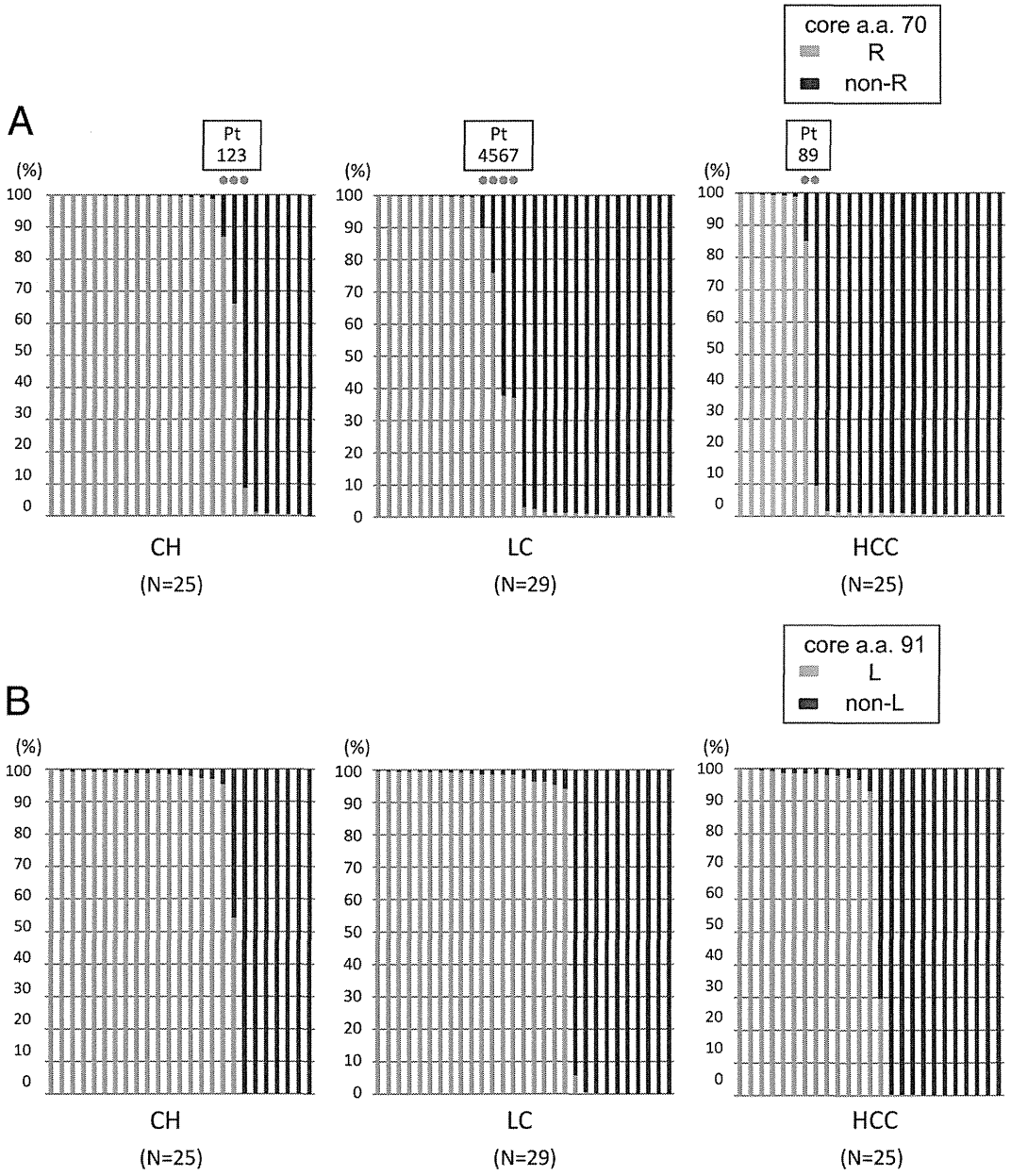

FIG 2 The core regions of the HCV genomes from 79 patients persistently infected with HCV genotype 1b (25 patients with chronic hepatitis [CH], 29 with liver cirrhosis [LC], and 25 with hepatocellular carcinoma [HCC]) were subjected to deep sequencing. Each bar represents the result for a single patient. At the specific locations of core aa 70 and aa 91, no single nucleotide mutation was observed in the previous control plasmid experiment. (A) Disease stages and percentages of mutations at core aa 70. Nine dots indicate the nine patients with a high mixture rate (between 5% and 95%) at core aa 70 (R and non-R). (B) Disease stages and percentages of mutations at core aa 91. (C) IL28B SNP and percentages of mutations at core aa 70. (D) IL28B SNP and percentages of mutations at core aa 91.

Since direct sequencing has also shown an association of several sites other than core aa 70 and 91 with the occurrence of HCC (6), those sites were also investigated for such an association. However, there was no clear relationship between these sites and disease progression, except for G209A (core aa R70Q) (see Fig. S1 and Table S2 in the supplemental material).

Phylogenetic tree analysis of HCV core region focusing on the core aa 70 residue. Because it was clear that the core aa 70 quasispecies state was significantly associated with disease progression, our next interest was to determine how this single hot spot is correlated with the remainder of the (almost-entire) core region. Therefore, phylogenetic tree analysis was performed, and genetic distances among aa 70-associated core sequences were also compared statistically. In constructing all phylogenetic trees, the three bases of the core 70 codon were removed, since the mutation rate of other parts of the core region is known to be rather low, and it was possible that the influence of the core aa 70 mutations might be overestimated in the phylogenetic trees.

At first, to determine the associations among the remainder of the core sequences across different patients, a phylogenetic tree was constructed for all 79 patients using dominant core sequences obtained from each patient. In constructing the tree, two domi-

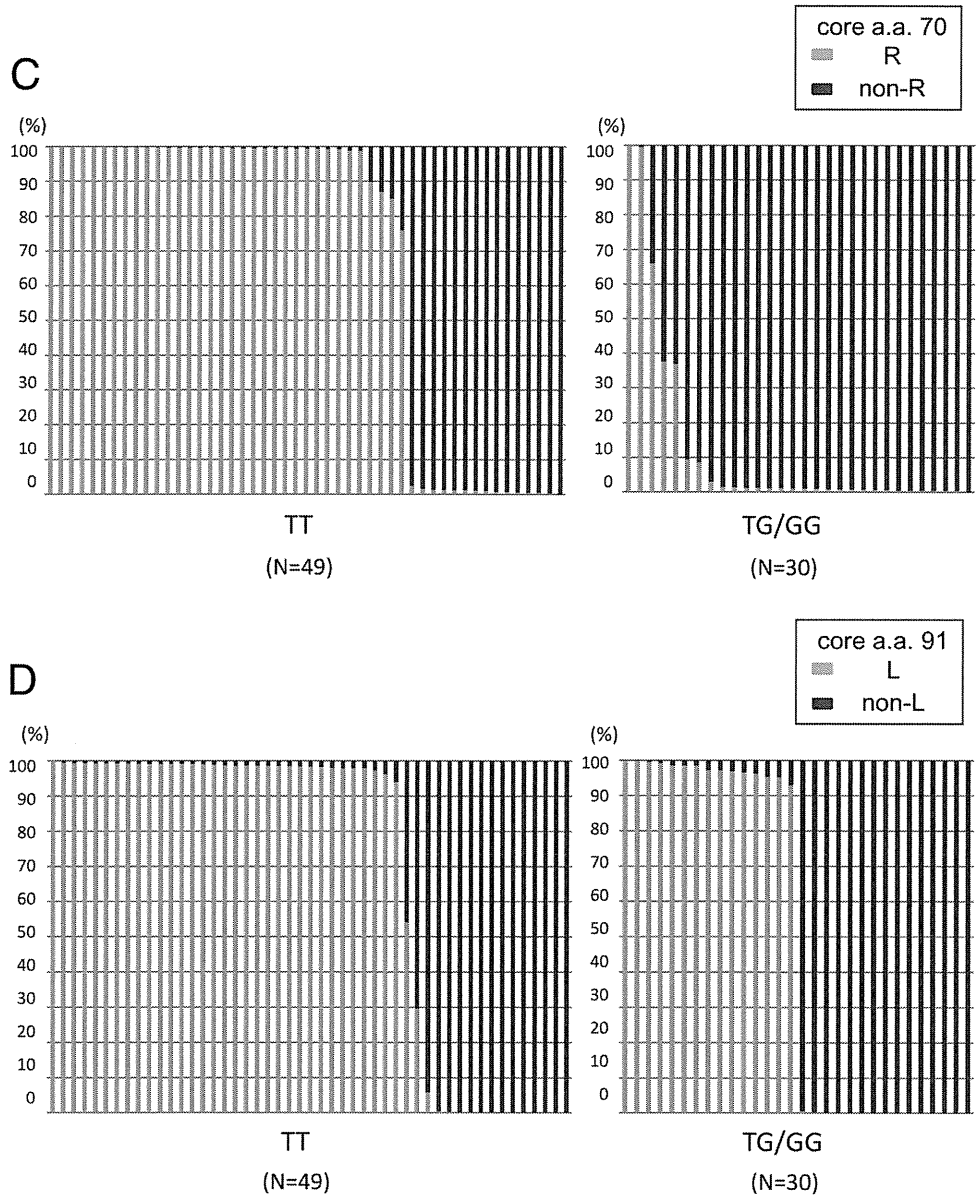

FIG 2 continued

nant sequences (the dominant core sequence in isolates with aa 70R and the dominant core sequence in isolates with aa 70non-R) were included in the analysis for each of the nine patients with high mixture rates (5% or more) of R and non-R at core aa 70 (Fig. 2A), while one dominant sequence each was included for other patients. As shown in Fig. 3A and Table 5, genetic distances calculated between every two core sequences with aa 70R (R-R) were significantly larger than those between two core sequences with aa 70non-R (non-R–non-R) or those between a

TABLE 3 Correlation between quasispecies composition and disease progression

Patient group (*n*)	Median % (range) with:	
	R at core aa 70[a]	L at core aa 91[b]
CH (25)	70.35 (0.00–100.00)	69.12 (0.00–99.40)
LC (29)	43.22 (0.24–100.00)	64.54 (0.00–99.50)
HCC (25)	28.20 (0.00–99.80)	52.23 (0.00–100.00)

[a] *P*, 0.018.
[b] *P*, 0.630.

TABLE 4 Correlation between quasispecies composition and IL28B SNP rs8099917

Group (sequence at IL28B SNP rs8099917)	Median % (range) with:	
	R at core aa 70[a]	L at core aa 91[b]
TT ($n = 49$)	68.15 (0.00–100.00)	68.24 (0.00–100.00)
TG/GG ($n = 30$)	12.64 (0.00–100.00)	48.76 (0.00–100.00)

[a] *P*, <0.005.
[b] *P*, 0.010.

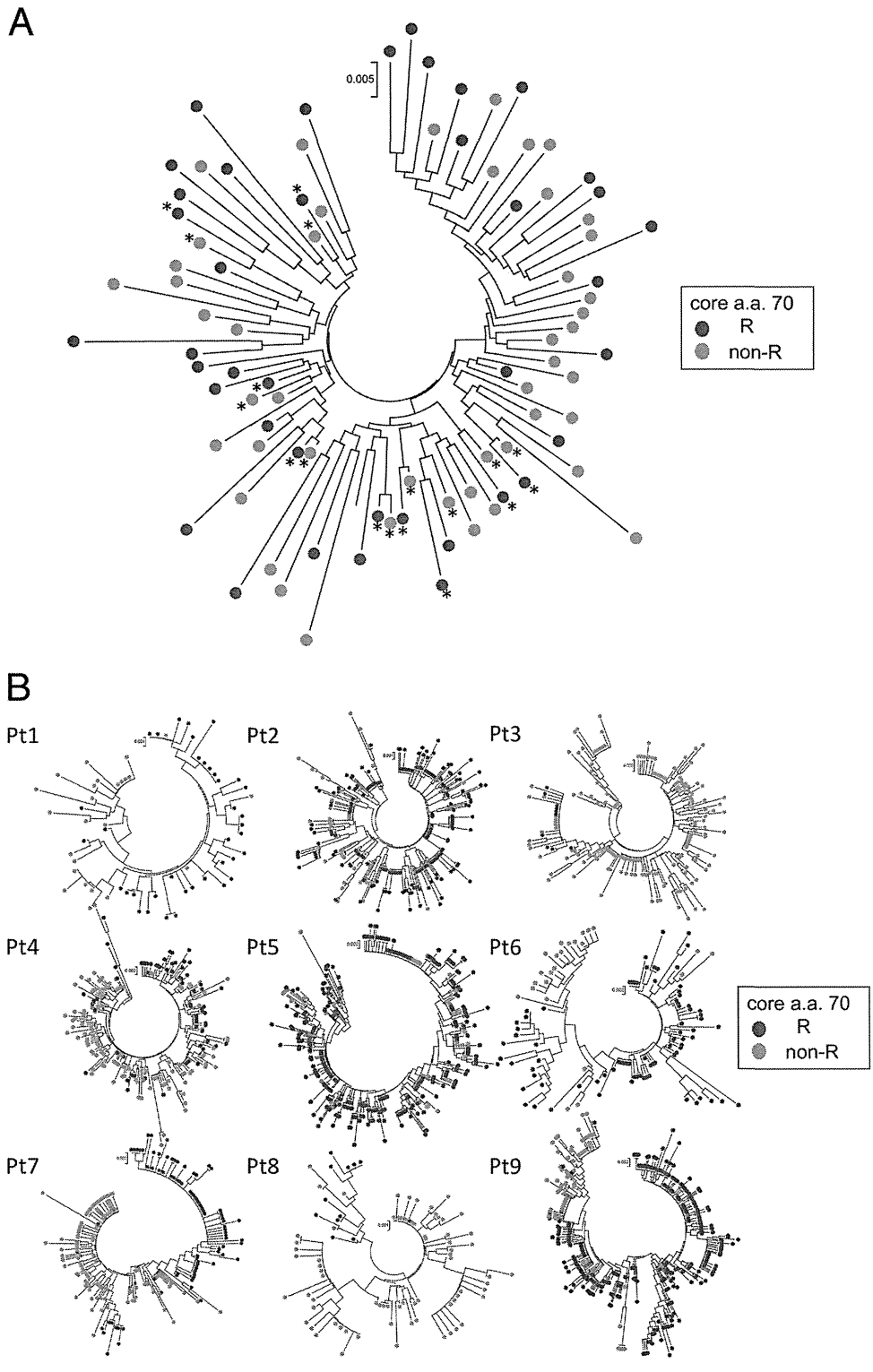

FIG 3 Phylogenetic trees were constructed using core sequences covering almost the entire core region. In the construction of those trees, the three bases of the core 70 codon were removed in the analysis of all 79 patients. Branches with core aa 70R are indicated by blue circles, while those with core aa 70non-R are indicated by pink circles. (A) Phylogenetic trees were constructed for all 79 patients by using dominant core sequences obtained from each patient. In the construction of the tree, two dominant sequences (a dominant core sequence in isolates with aa 70R and a dominant core sequence in isolates with aa 70non-R) were included in the analysis for each of the nine patients with high mixture rates (5% or more) of R and non-R at core aa 70 (Fig. 2A), while one dominant sequence each was included for other patients. (B) A phylogenetic tree of the core region was constructed for each patient with a high mixture rate (5% or more) of core aa 70R and core aa 70non-R. A total of nine patients were included in this analysis (patients 1 to 3 had CH; patients 4 to 7 had LC; and patients 9 and 10 had HCC). Pt, patient.

TABLE 5 Comparison of genetic distances among core subgroups related to aa 70 residues

Patient(s)[a]	Genetic distance (mean ± SD) between two core sequences[b]			Comparison of genetic distance measurements					
				Non-R–R vs non-R–non-R		Non-R–R vs R-R		Non-R–non-R vs R-R	
	Non-R–non-R	Non-R–R	R-R	Larger genetic distance	*P*	Larger genetic distance	*P*	Larger genetic distance	*P*
All (n = 79)	0.0349 ± 0.0101	0.0379 ± 0.0109	0.0401 ± 0.0113	Non-R–R	<0.001	R-R	<0.001	R-R	<0.001
CH									
Pt 1	0.0086 ± 0.0042	0.0098 ± 0.0037	0.0064 ± 0.0042	Non-R–R	<0.001	Non-R–R	<0.001	Non-R–non-R	<0.001
Pt 2	0.0097 ± 0.0048	0.0104 ± 0.0041	0.0087 ± 0.0038	Non-R–R	<0.001	Non-R–R	<0.001	Non-R–non-R	0.009
Pt 3	0.0107 ± 0.0058	0.0137 ± 0.0050	0.0034 ± 0.0022	Non-R–R	<0.001	Non-R–R	<0.001	Non-R–non-R	<0.001
LC									
Pt 4	0.0078 ± 0.0036	0.0103 ± 0.0038	0.0053 ± 0.0029	Non-R–R	<0.001	Non-R–R	<0.001	Non-R–non-R	<0.001
Pt 5	0.0118 ± 0.0090	0.0232 ± 0.0085	0.0159 ± 0.0170	Non-R–R	<0.001	Non-R–R	<0.001	No difference	0.991
Pt 6	0.0115 ± 0.0057	0.0121 ± 0.0055	0.0108 ± 0.0056	Non-R–R	<0.001	Non-R–R	<0.001	Non-R–non-R	<0.001
Pt 7	0.0141 ± 0.0085	0.0146 ± 0.0070	0.0136 ± 0.0067	Non-R–R	0.002	Non-R–R	<0.001	Non-R–non-R	<0.001
HCC									
Pt 8	0.0124 ± 0.0063	0.0225 ± 0.0060	0.0181 ± 0.0094	Non-R–R	<0.001	Non-R–R	<0.001	R-R	<0.001
Pt 9	0.0082 ± 0.0042	0.0162 ± 0.0047	0.0078 ± 0.0050	Non-R–R	<0.001	Non-R–R	<0.001	Non-R–non-R	<0.001

[a] Pt, patient.

[b] Non-R–non-R, comparison of two core sequences with residues other than R at aa 70; Non-R–R, comparison of a core sequence with a residue other than R at aa 70 and a core sequence with aa 70R; R-R, comparison of two core sequences with aa 70R. Genetic distances were calculated for all patients by using dominant sequences and for a single patient by using quasispecies sequences.

core sequence with aa 70R and a core sequence with aa 70non-R (non-R–R), demonstrating that core sequences with aa 70R were heterogeneous, while core sequences with aa 70non-R were homogeneous.

Next, to determine the association of the remainder of the core sequences in a single patient, phylogenetic trees were also constructed for each of the nine patients with high mixture rates (5% or more) of R and non-R residues at core aa 70 (Fig. 3B). As shown in Fig. 3B, HCV isolates with core aa 70R and those with core aa 70non-R formed distinctly clustered subgroups on the phylogenetic tree, according to the mutation status at core aa 70. Comparison of genetic distances also proved the finding that HCV isolates with core aa 70R and those with core aa 70non-R form distinctly clustered subgroups on the phylogenetic tree in a single patient, since genetic distances calculated between every two core sequences with aa 70R (R-R) or between every two core sequences with aa 70non-R (non-R–non-R) were significantly smaller than those between a core sequence with aa 70R and a core sequence with aa 70non-R (non-R–R). On the other hand, no significant difference was found when the genetic distance between two core sequences with aa 70non-R (non-R–non-R) and that between two core sequences with aa 70R (R-R) were compared in a single patient (Table 5).

Since the genetic relationships of the remainder of the core sequences were found to differ significantly according to the core aa 70 residue, we then investigated whether there are any common haplotypic sequences specific to each residue. In the comparison of dominant sequences in all 79 patients, most amino acid substitutions clustered in three amino acids (aa 70, aa 75, and aa 91) both in core sequences with aa 70R and in those with aa 70nonR, but no other substitutions specific to each core aa 70 residue were found (Fig. 4).

Quasispecies at core aa 70 and clinical characteristics. To clarify the association of the core aa 70 quasispecies with the clinical picture, levels of gamma-glutamyl transpeptidase (γ-GTP), albumin, platelets, and alpha-fetoprotein, as well as disease progression in the liver, were investigated for correlation with the core aa 70R/non-R mixture ratio. As shown in Fig. 5A and B, the values for these clinical parameters became significantly more abnormal as the proportion of non-R residues increased, showing that a high proportion of non-R residues at core aa 70 was significantly associated with disease severity and hepatocarcinogenesis.

DISCUSSION

This study examined, for the first time, the relationship between the progression of liver disease and the quasispecies nature of the HCV core region (already known to be associated with liver disease progression) by deep sequencing, with the focus on the core aa 70 residue. The analysis revealed that core aa 70 existed as a mixture of "mutant" Q/H (non-R) and "wild-type" R residues in most of the patients and that the proportion of mutant residues increased as liver disease advanced to LC and HCC. Meanwhile, phylogenetic analysis showed that the viral sequences of the almost-entire core region differed genetically depending on the status of core aa 70.

Before starting the analysis, we verified the rate of background error associated with the process of pyrosequencing by analyzing the control plasmid pCV-J4L6S (Fig. 1). Homopolymers of repeated bases, a weak point of pyrosequencing, were generated at two sites, with the same base appearing five and six times. The overall mutation rate at other sites was 0.092% ± 0.005%, and a mutation rate of 0.102% (mean + 2 SDs) or higher was defined as significant in the analysis, in order to avoid detecting background errors.

We focused our analysis on the quasispecies state of core aa 70,

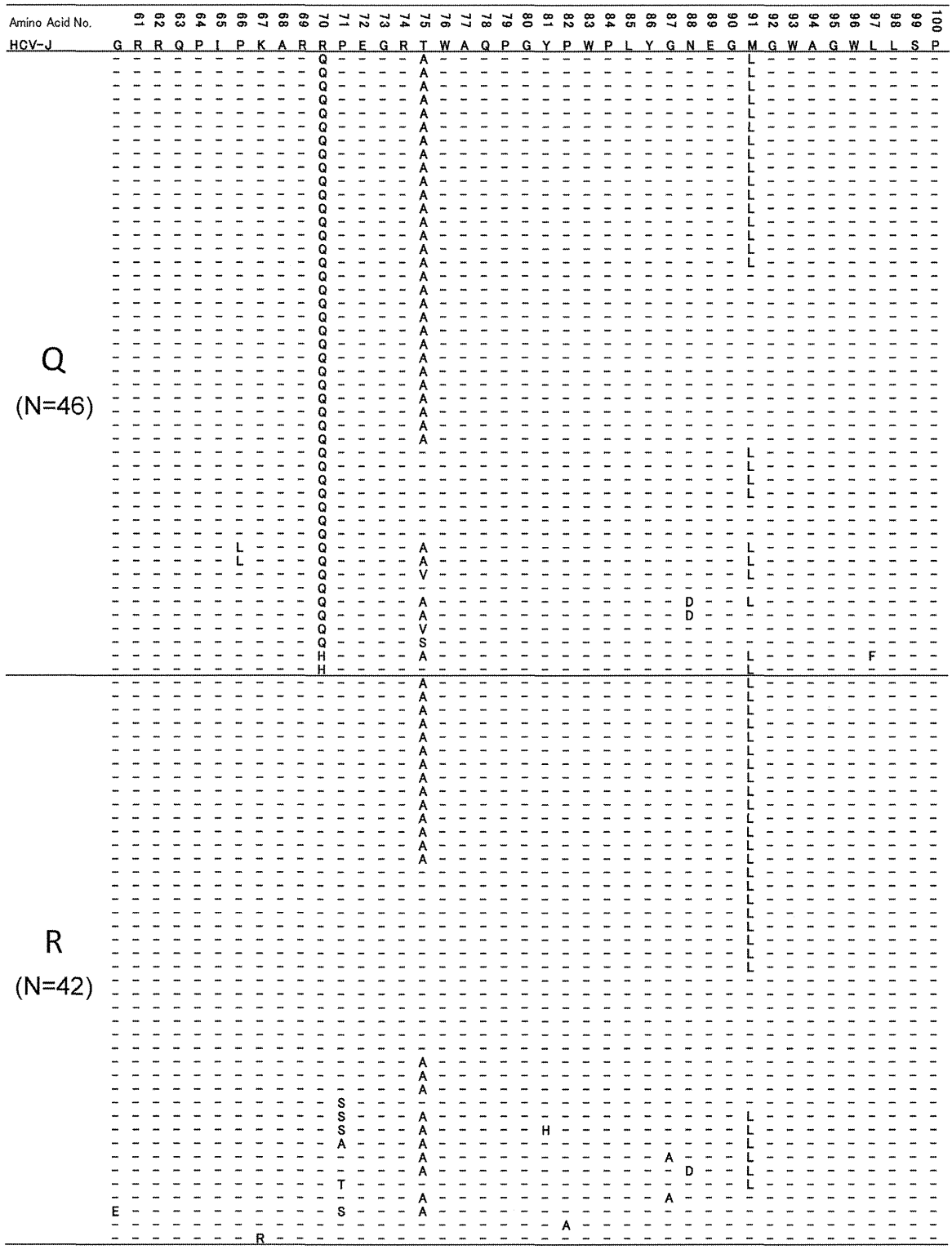

FIG 4 Dominant core amino acid haplotypic sequences dependent on the core aa 70 residues are given for all 79 patients. Two dominant sequences (a dominant core sequence in isolates with aa 70R and a dominant core sequence in isolates with aa 70non-R) were included for each of nine patients with high mixture rates (5% or more) of R and non-R at core aa 70, while one dominant sequence each was included for other patients. Therefore, a total of 88 haplotypic sequences are shown here. Since most amino acid mutations were observed in the limited core region, only that part of the core sequence is shown. The HCV-J isolate is used as the reference sequence for the core region.

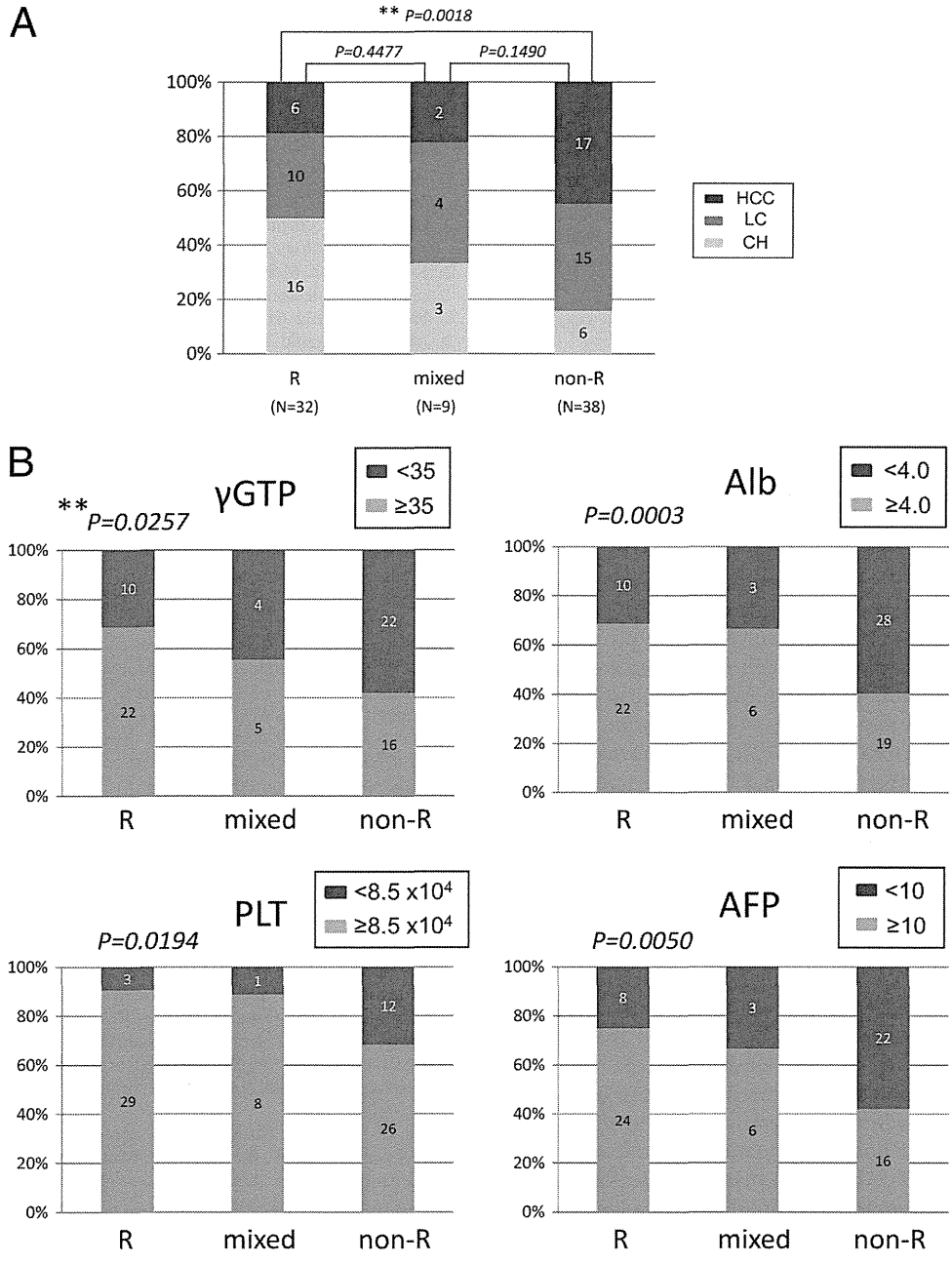

FIG 5 The advance of liver disease (A) and the levels of γ-GTP, albumin (Alb), platelets (PLT), and alpha-fetoprotein (AFP) (B) were investigated for correlation with the ratio of R to non-R at core aa 70. Results for R/R + non-R ratios of ≥95% (R), ≥5% and <95% (mixed), and <5% (non-R) are shown. **, Cochran-Armitage analysis.

because the presence of a quasispecies was expected at this position, considering reports by previous studies of its association with liver disease progression and the frequent observation of time-dependent changes (8, 9). R and non-R residues were mixed in 89.9% of the 79 patients examined in this study, indicating that the absence of a mixture was rare. Furthermore, the percentage of total isolates encoding non-R residues at this position showed a relationship with the advance of chronic liver disease, as shown in Fig. 2A and Table 3. Therefore, with regard to the relationship between the advance of liver disease and core aa 70, it may be accurate to say that a change in the ratio of amino acids at core aa 70, rather than mutation of core aa 70, was related to the advance of liver disease.

Because information for almost the entire core region was obtained from each patient, our next interest was to determine whether core aa 70 is associated with other viral regions. In other words, we sought to determine whether HCVs with core aa 70R and HCVs with core aa 70non-R are phylogenetically distinct variants. To clarify the issue, phylogenetic tree analysis using dominant sequences for the (almost-entire) core regions from all 79 patients was performed at first. This analysis disclosed, after the calculation of genetic distances, that core sequences with aa

70non-R were significantly more homogeneous than those with aa 70R, demonstrating that the hot spot core aa 70 residue is significantly associated with the remainder of the core sequence. Although the underlying mechanism is unclear, we speculated that the close correlation between core aa 70 residues and IL28B SNPs might have contributed to the result. That is, since endogenous IFN levels are known to be upregulated in patients with IL28B minor types (TG/GG) relative to those in patients with the IL28B major type (TT) in its natural state (28), it is possible that HCVs with core aa 70non-R, which are closely linked to IL28B TG/GG, are under strong antiviral pressure induced by IFN, resulting in the selection of more-homogeneous HCVs, which can survive in such an environment.

Considering this possibility, we proceeded to perform phylogenetic analyses of core sequences in single patients with high-percentage mixtures (5% or more) of R and non-R residues at core aa 70 by using deep-sequencing data, since the influence of endogenous IFNs was considered equal for all HCV isolates in a single patient. The deep-sequencing data showed that the genetic heterogeneity of core sequences in a single patient did not differ according to the core aa 70 residue but that core sequences formed distinct subgroups on the phylogenetic tree according to the core aa 70 residue (Fig. 3B), and this result was also proved by the calculation of genetic distances (Table 5). However, since no common haplotypic sequences specific to each residue at core aa 70 were found across the patients (Fig. 4), we cannot determine whether core aa 70R and aa 70non-R HCVs are phylogenetically distinct variants. It is possible that the result simply reflects a major evolutional event of core aa 70 mutations followed by derivative variants; however, extension of the investigation and analysis to viral regions beyond the core region might reveal such associations. However, due to the technical limitations of second-generation sequencers, deep-sequencing analysis of the long amplicon is difficult, and new technology is needed.

With regard to the mechanism underlying the relationship between the core protein and disease progression and hepatocarcinogenesis, a study using transgenic mice showed that the core protein induces HCC (29). Fat metabolism was accelerated in the liver, leading to inflammation, iron metabolism, oxidative stress, and insulin resistance, which were considered to be the carcinogenic factors (30–32). Clinically, mutation of the core and the concentration of γ-GTP in serum, a marker of steatosis, are related, and the relationship between IL28B SNP and liver steatosis or γ-GTP has been elucidated (33). In this study, moreover, we have confirmed the correlation between the core aa 70 mixture ratio, determined by deep-sequencing analysis, and clinical parameters reflecting disease progression, illustrating the significant association of core aa 70 with disease progression (Fig. 5A and B).

In conclusion, the quasispecies state of the core region was analyzed by deep sequencing. It was found that the status of the quasispecies was closely related to the advance of HCV-associated liver disease. In order to understand the mechanism of hepatocarcinogenesis, it is desirable to elucidate pathogenesis further by detailed examination of the quasispecies of the HCV core gene.

ACKNOWLEDGMENTS

Nobuyuki Enomoto received research funding from MSD (Tokyo, Japan) and Roche (Tokyo, Japan).

This study was supported in part by grants-in-aid from the Ministry of Education, Science, Sports and Culture of Japan (grants 23390195, 23791404, 24590964, and 24590965) and in part by grants-in-aid from the Ministry of Health, Labour, and Welfare of Japan (H23-kanen-001, H23-kanen-004, H23-kanen-006, H24-kanen-002, H24-kanen-004, and H25-kanen-006).

REFERENCES

1. Niederau C, Lange S, Heintges T, Erhardt A, Buschkamp M, Hurter D, Nawrocki M, Kruska L, Hensel F, Petry W, Haussinger D. 1998. Prognosis of chronic hepatitis C: results of a large, prospective cohort study. Hepatology 28:1687–1695.
2. Koike K. 2005. Molecular basis of hepatitis C virus-associated hepatocarcinogenesis: lessons from animal model studies. Clin. Gastroenterol. Hepatol. 3:S132–S135.
3. Akuta N, Suzuki F, Sezaki H, Suzuki Y, Hosaka T, Someya T, Kobayashi M, Saitoh S, Watahiki S, Sato J, Matsuda M, Arase Y, Ikeda K, Kumada H. 2005. Association of amino acid substitution pattern in core protein of hepatitis C virus genotype 1b high viral load and non-virological response to interferon-ribavirin combination therapy. Intervirology 48:372–380.
4. Akuta N, Suzuki F, Hirakawa M, Kawamura Y, Sezaki H, Suzuki Y, Hosaka T, Kobayashi M, Saitoh S, Arase Y, Ikeda K, Kumada H. 2011. Amino acid substitutions in hepatitis C virus core region predict hepatocarcinogenesis following eradication of HCV RNA by antiviral therapy. J. Med. Virol. 83:1016–1022.
5. Akuta N, Suzuki F, Kawamura Y, Yatsuji H, Sezaki H, Suzuki Y, Hosaka T, Kobayashi M, Arase Y, Ikeda K, Kumada H. 2007. Amino acid substitutions in the hepatitis C virus core region are the important predictor of hepatocarcinogenesis. Hepatology 46:1357–1364.
6. Fishman SL, Factor SH, Balestrieri C, Fan X, Dibisceglie AM, Desai SM, Benson G, Branch AD. 2009. Mutations in the hepatitis C virus core gene are associated with advanced liver disease and hepatocellular carcinoma. Clin. Cancer Res. 15:3205–3213.
7. Nakamoto S, Imazeki F, Fukai K, Fujiwara K, Arai M, Kanda T, Yonemitsu Y, Yokosuka O. 2010. Association between mutations in the core region of hepatitis C virus genotype 1 and hepatocellular carcinoma development. J. Hepatol. 52:72–78.
8. Akuta N, Suzuki F, Seko Y, Kawamura Y, Sezaki H, Suzuki Y, Hosaka T, Kobayashi M, Hara T, Saitoh S, Arase Y, Ikeda K, Kumada H. 2012. Complicated relationships of amino acid substitution in hepatitis C virus core region and IL28B genotype influencing hepatocarcinogenesis. Hepatology 56:2134–2141.
9. Miura M, Maekawa S, Kadokura M, Sueki R, Komase K, Shindo H, Ohmori T, Kanayama A, Shindo K, Amemiya F, Nakayama Y, Kitamura T, Uetake T, Inoue T, Sakamoto M, Okada S, Enomoto N. 2012. Analysis of viral amino acids sequences and the IL28B SNP influencing the development of hepatocellular carcinoma in chronic hepatitis C. Hepatol. Int. 6:386–396.
10. Ge D, Fellay J, Thompson AJ, Simon JS, Shianna KV, Urban TJ, Heinzen EL, Qiu P, Bertelsen AH, Muir AJ, Sulkowski M, McHutchison JG, Goldstein DB. 2009. Genetic variation in IL28B predicts hepatitis C treatment-induced viral clearance. Nature 461:399–401.
11. Rauch A, Kutalik Z, Descombes P, Cai T, Di Iulio J, Mueller T, Bochud M, Battegay M, Bernasconi E, Borovicka J, Colombo S, Cerny A, Dufour JF, Furrer H, Gunthard HF, Heim M, Hirschel B, Malinverni R, Moradpour D, Mullhaupt B, Witteck A, Beckmann JS, Berg T, Bergmann S, Negro F, Telenti A, Bochud PY. 2010. Genetic variation in *IL28B* is associated with chronic hepatitis C and treatment failure: a genome-wide association study. Gastroenterology 138:1338–1345.e7.
12. Suppiah V, Moldovan M, Ahlenstiel G, Berg T, Weltman M, Abate ML, Bassendine M, Spengler U, Dore GJ, Powell E, Riordan S, Sheridan D, Smedile A, Fragomeli V, Muller T, Bahlo M, Stewart GJ, Booth DR, George J. 2009. IL28B is associated with response to chronic hepatitis C interferon-alpha and ribavirin therapy. Nat. Genet. 41:1100–1104.
13. Tanaka Y, Nishida N, Sugiyama M, Kurosaki M, Matsuura K, Sakamoto N, Nakagawa M, Korenaga M, Hino K, Hige S, Ito Y, Mita E, Tanaka E, Mochida S, Murawaki Y, Honda M, Sakai A, Hiasa Y, Nishiguchi S, Koike A, Sakaida I, Imamura M, Ito K, Yano K, Masaki N, Sugauchi F, Izumi N, Tokunaga K, Mizokami M. 2009. Genome-wide association of IL28B with response to pegylated interferon-alpha and ribavirin therapy for chronic hepatitis C. Nat. Genet. 41:1105–1109.
14. Bochud PY, Bibert S, Kutalik Z, Patin E, Guergnon J, Nalpas B, Goossens N, Kuske L, Mullhaupt B, Gerlach T, Heim MH, Moradpour

D, Cerny A, Malinverni R, Regenass S, Dollenmaier G, Hirsch H, Martinetti G, Gorgiewski M, Bourliere M, Poynard T, Theodorou I, Abel L, Pol S, Dufour JF, Negro F. 2012. IL28B alleles associated with poor hepatitis C virus (HCV) clearance protect against inflammation and fibrosis in patients infected with non-1 HCV genotypes. Hepatology 55: 384–394.

15. Fabris C, Falleti E, Cussigh A, Bitetto D, Fontanini E, Bignulin S, Cmet S, Fornasiere E, Fumolo E, Fangazio S, Cerutti A, Minisini R, Pirisi M, Toniutto P. 2011. IL-28B rs12979860 C/T allele distribution in patients with liver cirrhosis: role in the course of chronic viral hepatitis and the development of HCC. J. Hepatol. 54:716–722.
16. Joshita S, Umemura T, Katsuyama Y, Ichikawa Y, Kimura T, Morita S, Kamijo A, Komatsu M, Ichijo T, Matsumoto A, Yoshizawa K, Kamijo N, Ota M, Tanaka E. 2012. Association of IL28B gene polymorphism with development of hepatocellular carcinoma in Japanese patients with chronic hepatitis C virus infection. Hum. Immunol. 73:298–300.
17. Marabita F, Aghemo A, De Nicola S, Rumi MG, Cheroni C, Scavelli R, Crimi M, Soffredini R, Abrignani S, De Francesco R, Colombo M. 2011. Genetic variation in the interleukin-28B gene is not associated with fibrosis progression in patients with chronic hepatitis C and known date of infection. Hepatology 54:1127–1134.
18. Pawlotsky JM. 2006. Hepatitis C virus population dynamics during infection. Curr. Top. Microbiol. Immunol. 299:261–284.
19. Hiraga N, Imamura M, Abe H, Hayes CN, Kono T, Onishi M, Tsuge M, Takahashi S, Ochi H, Iwao E, Kamiya N, Yamada I, Tateno C, Yoshizato K, Matsui H, Kanai A, Inaba T, Tanaka S, Chayama K. 2011. Rapid emergence of telaprevir resistant hepatitis C virus strain from wild-type clone in vivo. Hepatology 54:781–788.
20. Nasu A, Marusawa H, Ueda Y, Nishijima N, Takahashi K, Osaki Y, Yamashita Y, Inokuma T, Tamada T, Fujiwara T, Sato F, Shimizu K, Chiba T. 2011. Genetic heterogeneity of hepatitis C virus in association with antiviral therapy determined by ultra-deep sequencing. PLoS One 6:e24907. doi:10.1371/journal.pone.0024907.
21. Verbinnen T, Van Marck H, Vandenbroucke I, Vijgen L, Claes M, Lin TI, Simmen K, Neyts J, Fanning G, Lenz O. 2010. Tracking the evolution of multiple *in vitro* hepatitis C virus replicon variants under protease inhibitor selection pressure by 454 deep sequencing. J. Virol. 84:11124–11133.
22. Wang GP, Sherrill-Mix SA, Chang KM, Quince C, Bushman FD. 2010. Hepatitis C virus transmission bottlenecks analyzed by deep sequencing. J. Virol. 84:6218–6228.
23. Nagayama K, Kurosaki M, Enomoto N, Maekawa SY, Miyasaka Y, Tazawa J, Izumi N, Marumo F, Sato C. 1999. Time-related changes in full-length hepatitis C virus sequences and hepatitis activity. Virology 263: 244–253.
24. Gates AT, Sarisky RT, Gu B. 2004. Sequence requirements for the development of a chimeric HCV replicon system. Virus Res. 100:213–222.
25. Tamura K, Peterson D, Peterson N, Stecher G, Nei M, Kumar S. 2011. MEGA5: molecular evolutionary genetics analysis using maximum likelihood, evolutionary distance, and maximum parsimony methods. Mol. Biol. Evol. 28:2731–2739.
26. Becker EA, Burns CM, Leon EJ, Rajabojan S, Friedman R, Friedrich TC, O'Connor SL, Hughes AL. 2012. Experimental analysis of sources of error in evolutionary studies based on Roche/454 pyrosequencing of viral genomes. Genome Biol. Evol. 4:457–465.
27. Quince C, Lanzen A, Curtis TP, Davenport RJ, Hall N, Head IM, Read LF, Sloan WT. 2009. Accurate determination of microbial diversity from 454 pyrosequencing data. Nat. Methods 6:639–641.
28. Honda M, Sakai A, Yamashita T, Nakamoto Y, Mizukoshi E, Sakai Y, Nakamura M, Shirasaki T, Horimoto K, Tanaka Y, Tokunaga K, Mizokami M, Kaneko S. 2010. Hepatic ISG expression is associated with genetic variation in interleukin 28B and the outcome of IFN therapy for chronic hepatitis C. Gastroenterology 139:499–509.
29. Moriya K, Fujie H, Shintani Y, Yotsuyanagi H, Tsutsumi T, Ishibashi K, Matsuura Y, Kimura S, Miyamura T, Koike K. 1998. The core protein of hepatitis C virus induces hepatocellular carcinoma in transgenic mice. Nat. Med. 4:1065–1067.
30. Leandro G, Mangia A, Hui J, Fabris P, Rubbia-Brandt L, Colloredo G, Adinolfi LE, Asselah T, Jonsson JR, Smedile A, Terrault N, Pazienza V, Giordani MT, Giostra E, Sonzogni A, Ruggiero G, Marcellin P, Powell EE, George J, Negro F. 2006. Relationship between steatosis, inflammation, and fibrosis in chronic hepatitis C: a meta-analysis of individual patient data. Gastroenterology 130:1636–1642.
31. Nishina S, Hino K, Korenaga M, Vecchi C, Pietrangelo A, Mizukami Y, Furutani T, Sakai A, Okuda M, Hidaka I, Okita K, Sakaida I. 2008. Hepatitis C virus-induced reactive oxygen species raise hepatic iron level in mice by reducing hepcidin transcription. Gastroenterology 134:226–238.
32. Okuda M, Li K, Beard MR, Showalter LA, Scholle F, Lemon SM, Weinman SA. 2002. Mitochondrial injury, oxidative stress, and antioxidant gene expression are induced by hepatitis C virus core protein. Gastroenterology 122:366–375.
33. Abe H, Ochi H, Maekawa T, Hayes CN, Tsuge M, Miki D, Mitsui F, Hiraga N, Imamura M, Takahashi S, Ohishi W, Arihiro K, Kubo M, Nakamura Y, Chayama K. 2010. Common variation of IL28 affects γ-GTP levels and inflammation of the liver in chronically infected hepatitis C virus patients. J. Hepatol. 53:439–443.

Vaccine 31 (2013) 3199–3205

Contents lists available at SciVerse ScienceDirect

Vaccine

journal homepage: www.elsevier.com/locate/vaccine

Effects of immunization of pregnant guinea pigs with guinea pig cytomegalovirus glycoprotein B on viral spread in the placenta

Kaede Hashimoto[a,b], Souichi Yamada[a], Harutaka Katano[c], Saki Fukuchi[a,b], Yuko Sato[c], Minami Kato[a], Toyofumi Yamaguchi[d], Kohji Moriishi[b], Naoki Inoue[a,*]

[a] Department of Virology I, National Institute of Infectious Diseases, Tokyo, Japan
[b] Department of Microbiology, School of Medicine, University of Yamanashi, Yamanashi, Japan
[c] Department of Pathology, National Institute of Infectious Diseases, Tokyo, Japan
[d] Department of Biosciences, Teikyo University of Science, Yamanashi, Japan

ARTICLE INFO

Article history:
Received 5 March 2013
Accepted 24 April 2013
Available online 15 May 2013

Keywords:
Cytomegalovirus
Congenital infection
Animal model
Placenta
Glycoprotein B
Vaccine

ABSTRACT

Background: Cytomegalovirus (CMV) is the most common cause of congenital virus infection. Infection of guinea pigs with guinea pig CMV (GPCMV) can provide a useful model for the analysis of its pathogenesis as well as for the evaluation of vaccines. Although glycoprotein B (gB) vaccines have been reported to reduce the incidence and mortality of congenital infection in human clinical trials and guinea pig animal models, the mechanisms of protection remain unclear.
Methods: To understand the gB vaccine protection mechanisms, we analyzed the spread of challenged viruses in the placentas and fetuses of guinea pig dams immunized with recombinant adenoviruses expressing GPCMV gB and β-galactosidase, rAd-gB and rAd-LacZ, respectively.
Results: Mean body weight of the fetuses in the dams immunized with rAd-LacZ followed by GPCMV challenge 3 weeks after immunization was 78% of that observed for dams immunized with rAd-gB. Under conditions in which congenital infection occurred in 75% of fetuses in rAd-LacZ-immunized dams, only 13% of fetuses in rAd-gB-immunized dams were congenitally infected. The placentas were infected less frequently in the gB-immunized animals. In the placentas of the rAd-LacZ- and rAd-gB-immunized animals, CMV early antigens were detected mainly in the spongiotrophoblast layer. Focal localization of viral antigens in the spongiotrophoblast layer suggests cell-to-cell viral spread in the placenta. In spite of a similar level of antibodies against gB and avidity indices among fetuses in each gB-immunized dam, congenital infection was sometimes observed in a littermate fetus. In such infected fetuses, CMV spread to most organs.
Conclusions: Our results suggest that antibodies against gB protected against infection mainly at the interface of the placenta rather than from the placenta to the fetus. The development of strategies to block cell-to-cell viral spread in the placenta is, therefore, required for effective protection against congenital CMV infection.

1. Introduction

Human cytomegalovirus (HCMV) is the most common cause of congenital virus infection. Congenital infection occurs in 0.2–1% of all births, and causes birth defects and developmental abnormalities, including sensorineural hearing loss (SNHL) and developmental delay [1–3]. Since one of the major routes of transmission to pregnant mothers is suggested to be *via* the excretions of their own children [4,5], development of a vaccine is the only effective way for protection against primary HCMV infection. Indeed, a review panel from the Institute of Medicine indicated that the development of a vaccine against HCMV, particularly with the aim of preventing primary infection in pregnant women, was of the highest priority among those for infectious diseases other than HIV [6]. As one of the promising approaches, purified glycoprotein B (gB) protein in combination with the MF59 adjuvant was used for a phase 2 clinical trial on CMV-seronegative women who had recently delivered a child and had intention of having another, and this subunit gB vaccine protocol demonstrated 50% efficacy against primary infection [7]. Although such results are encouraging, further studies are required to improve the efficacy and rapid waning of protection.

Animal models are generally valuable in gaining a better understanding of pathogenesis as well as in developing therapeutics for

* Corresponding author at: Laboratory of Herpesviruses, Department of Virology I, National Institute of Infectious Diseases, 1-23-1 Toyama, Shinjuku-ku, Tokyo 162-8640, Japan. Tel.: +81 3 4582 2663; fax: +81 3 5285 1180.
E-mail address: ninoue@nih.go.jp (N. Inoue).

0264-410X/$ – see front matter © 2013 Elsevier Ltd. All rights reserved.
http://dx.doi.org/10.1016/j.vaccine.2013.04.078

infectious diseases. In contrast to murine and rat CMVs, guinea pig CMV (GPCMV) crosses the placenta and causes infection *in utero*. Importantly, congenital GPCMV infection causes diseases similar to congenital HCMV diseases, such as IUGR and labyrinthitis [8–11]. Previous studies using a guinea pig model demonstrated that congenital infection and mortality in pups were reduced by the administration of anti-gB antibodies [12] or by immunization with gB in the form of a DNA or purified subunit vaccine [13,14]. In the placenta, GPCMV-induced histopathological lesions with viral antigens were localized at the transitional zone between the capillarized labyrinth and the noncapillarized interlobium [15]. However, the mechanism by which gB immunization inhibits such viral spread in the placenta and fetus remains unclear. In this study, to better understand the mechanism, we analyzed the spread of viruses in the placentas and fetuses of gB-immunized dams after virus challenge.

2. Materials and methods

2.1. Cells and viruses

Guinea pig lung fibroblasts (GPL, ATCC) were initially cultured in F-12 medium supplemented with 10% fetal bovine serum (FBS) and subsequently, after infection with GPCMV, in F-12 medium supplemented with 2% FBS. GPL cells were infected with a GPCMV (strain 22122) stock purchased from ATCC. Salivary glands (SGs) of a guinea pig (Hartley strain) infected with the original GPCMV stock were recovered, minced, sonicated briefly, and then centrifuged to remove debris. The supernatant (SG-P0) was used for the infection of GPL cells, and viral stocks were prepared after propagation of the cell-free virus 5 times in GPL cells (SG-P5). Virus stocks were concentrated by ultracentrifugation (82,000 × *g* for 2 h) in a 20% sucrose step gradient. Infectious units (IUs) of the stocks were determined by immunostaining of GPL cells infected with the diluted stocks in 12- or 24-well plates and cultured for 2–3 days as described previously [16].

A recombinant GPCMV expressing red fluorescent protein (RFP) was prepared as follows: The sequence region from position 4244 to 8013 (positions are based on Ref. [17]) of GPCMV (SG-P5) was replaced with a 1.8-kb DNA fragment covering the TurboRFP gene under the control of the CMV IE promoter (Evorgen JSC, Russia) by homologous recombination in GPL cells. The RFP-expressing GPCMV candidates were then plaque-purified several times in GPL cells. One of the candidates, GPCMV-RFP(4A), was used for neutralization assay.

2.2. Recombinant adenoviral vectors

The gene encoding the extracellular domain (amino acids 1–674) of GPCMV gB (rAd-gB) and the LacZ gene encoding β-galactosidase were cloned into a pENTR-3C vector and then into pAd/CMV/V5/DEST by using the LR recombinase system (Invitrogen), resulting in pAd-gB and pAd-LacZ, respectively. Recombinant adenoviruses, rAd-gB and rAd-LacZ, were recovered by transfection of 293A cells with pAd-gB and with pAd-LacZ, respectively, amplified, and purified by centrifugation through two CsCl step gradients as described previously [18].

2.3. Animal studies

Female guinea pigs at the indicated weeks after birth (Hartley, Japan SLC, Inc.) were inoculated intraperitonealy (i.p.) with 10^6 IUs of GPCMV and euthanized 3-weeks later. Blood specimens were drawn directly from the heart, and organ specimens, including liver, spleen, kidney, lung, and salivary gland, were harvested. Dams at 1-week of gestation (Japan SLC, Inc.) were inoculated i.p. with 10^{10} transducing units (TUs) of rAd viruses, infected subcutaneously with 10^6 IUs of GPCMV (SG-P5) 3-weeks after the inoculation, and euthanized 3-weeks later. Blood specimens were drawn from the dams and their fetuses. Salivary glands were also obtained from the dams. The placentas and fetuses were weighed and organs were harvested from the fetuses. All animal procedures were approved by the Animal Care and Use Committee of the National Institute of Infectious Diseases (NIID), and were conducted according to the 'Guidelines for Animal Experiments Performed at the NIID'.

2.4. Immunological assays

Transfection was performed by using a commercial reagent (Fugene6, Roche). GPCMV-infected and -transfected cells were fixed with acetone for 5 min and expression of antigens were examined by an immunofluorescence assay as described previously [19].

Anti-gB antibody levels in the dams and fetuses were measured by ELISA using the cytoplasmic fraction (0.8 μg of protein/well) of 293T cells transfected with a gB construct. Absorbance values obtained using sera diluted at 1:200 had a good correlation with titers determined as a maximum dilution (in a range of 1:200–3200) that gives the threshold absorbance (data not shown). Avidity indices of anti-gB IgG were determined by a 10-min treatment with 4 M urea.

Neutralizing activities in sera were measured as follows. A total of 1×10^4 IUs of GPCMV-RFP(4A) in 50 μl of medium was mixed with 50 μl of serially diluted serum specimens, and incubated at 37 °C for 1 h. The reaction mixtures were then diluted and inoculated into GPL cell cultures. RFP-positive foci were counted 3 days after infection.

2.5. Immunohistochemistry

All organs obtained from sacrificed animals were fixed in 10% buffered formalin. Formalin-fixed specimens were embedded in paraffin, sectioned, and stained with hematoxylin and eosin (HE), as described previously [8]. Immunohistochemical analysis was performed using the monoclonal antibody g-1, which detects a GPCMV early antigen, or the rabbit polyclonal antibody against immediate-early proteins 1 and 2, which was generated by the immunization of rabbits with a GST-IE1/2 fusion protein, as primary antibodies. For the second- and third-phase immunostaining reagents, a biotinylated $F(ab')_2$ fragment of rabbit anti-mouse immunoglobulin (DAKO) or of goat anti-rabbit immunoglobulin (DAKO) and peroxidase-conjugated streptavidin (DAKO) were used. DAB was used as a chromogen and the slides were counterstained with hematoxylin.

2.6. Quantification of viral DNA

DNA samples were prepared from the placentas and fetal organs, and viral DNAs in the samples were detected by real-time PCR assays for GPCMV GP83 and β-actin genes as described previously [16].

2.7. Statistical analysis

Mann–Whitney *U* test was used to analyze statistical differences in the weight of animals, fetuses, and placentas, and in the number of viral foci in placentas. Chi-square test was also used to analyze differences in the rates of CMV-positive placentas and fetal organs.

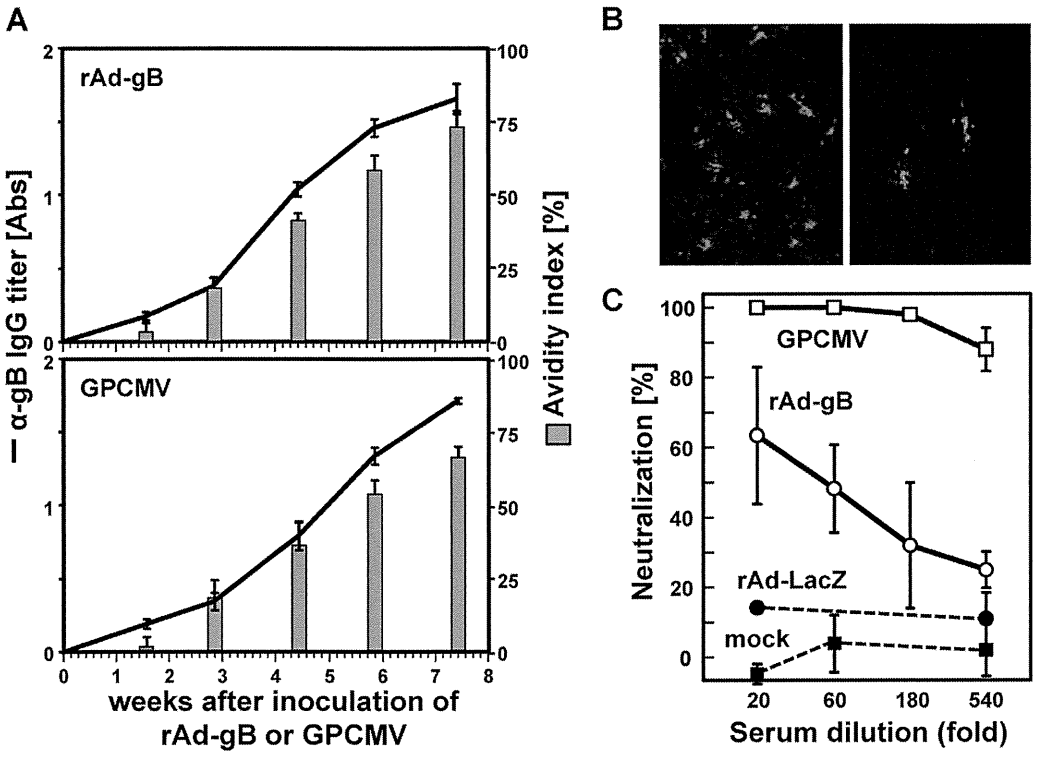

Fig. 1. Induction of anti-gB antibodies by immunization with rAd-gB. (A) Three 4-week old guinea pigs were inoculated with 10^{10} TUs of rAd-gB and GPCMV, respectively. Blood specimens were drawn from the great saphenous vein at the indicated days after inoculation, and their anti-gB IgG titers and avidity indices were measured. (B) RFP-expressing GPCMV, GPCMV-RFP(4A), was used for the detection of neutralizing antibodies. Examples of RFP foci detected in GPL cells after treatment of the virus with sera obtained from the mock-infected (left) and GPCMV-infected (right) animals are shown. (C) Neutralization assay was performed at indicated serum dilutions in triplicate. Serum specimens obtained from 3 guinea pigs immunized with rAd-gB and rAd-LacZ 7-weeks after immunization were analyzed and the averages and SDs of neutralization (%) by the respective 3 specimens are plotted. No reduction and complete inhibition of RFP-positive foci are indicated as 0% and 100% neutralization, respectively. Sera obtained from mock- and GPCMV-infected guinea pigs were used as negative and positive controls, respectively, for the detection of neutralizing antibodies.

3. Results

3.1. gB immunization of young animals

Administration of 10^{10} TUs of rAd-gB to young guinea pigs induced anti-gB antibodies, and the avidity index for the anti-gB antibodies increased gradually (Fig. 1A). Neutralizing activities against GPCMV in sera were measured by using RFP-expressing GPCMV (Fig. 1B and C). Although the anti-gB IgG titers and avidity indices of sera obtained from the animals immunized with rAd-gB were at a level similar to those of sera obtained from the animals infected with GPCMV (SG-P5), the neutralizing activities of the former sera were weaker than those of the latter sera, suggesting the presence of neutralizing antibodies other than those against gB.

Next, young animals were inoculated with rAd-gB or rAd-LacZ, and challenged with GPCMV at 2- to 4-weeks after inoculation. Although the GPCMV challenge resulted in a short-term weight loss of 6–17% in the rAd-LacZ-inoculated control animals, gB immunization suppressed weight loss (Fig. 2). It seems that younger animals are more prone to body weight loss after virus challenge. In addition, the amount of viral DNA in the salivary glands in the rAd-gB-inoculated animals was less than 1% that in the rAd-LacZ-inoculated animals (data not shown), indicating that gB immunization reduced viral dissemination to the salivary glands.

3.2. Protection of the placentas and fetuses against infection in gB-immunized dams

We observed that viral antigens and DNA were rarely detected in the placenta 1-week after infection at 4-weeks of gestation, but

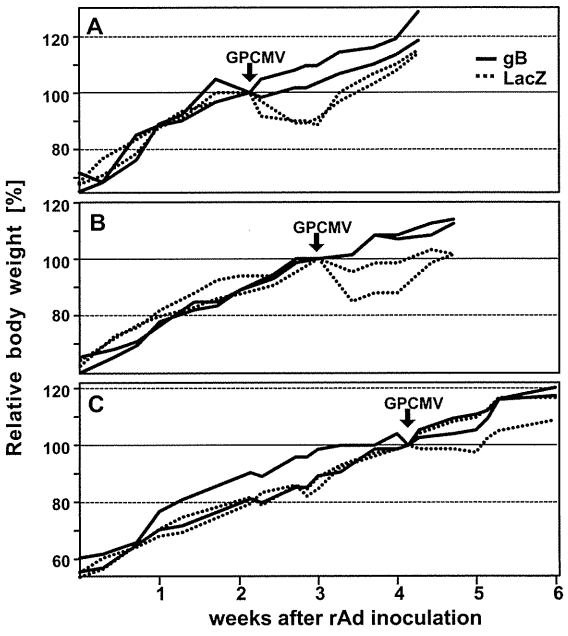

Fig. 2. Relative body weights of animals immunized with rAd-gB (continuous lines) and with rAd-LacZ (dashed lines) followed by GPCMV challenge (arrows) at 2-weeks (A), 3-weeks (B) and 4-weeks (C) after immunization are shown by using the weight of each animal at the time of the challenge as a 100% control.